



Published in final edited form as:

J Med Chem. 2016 April 28; 59(8): 3635–3649. doi:10.1021/acs.jmedchem.5b01718.

Repurposing the Clinically Efficacious Anti-Fungal Agent Itraconazole as an Anti-Cancer Chemotherapeutic

Jennifer R. Pace^{‡,§}, Albert M. DeBerardinis^{‡,§}, Vibhavari Sail[§], Silvia K. Tacheva-Grigorova[¥], Kelly A. Chan[§], Raymond Tran[§], Daniel S. Raccuia[§], Robert J. Wechsler-Reya[¥], and M. Kyle Hadden^{§,*}

[§]Department of Pharmaceutical Sciences, University of Connecticut, 69 N Eagleville Rd, Unit 3092, Storrs, CT 06269-3092

[¥]Tumor Initiation and Maintenance Program, NCI-Designated Cancer Center, Sanford Burnham Prebys Medical Discovery Institute, 2880 Torrey Pines Scenic Drive, La Jolla, CA 92037

Abstract

Itraconazole (ITZ) is an FDA-approved member of the triazole class of anti-fungal agents. Two recent drug repurposing screens identified ITZ as a promising anti-cancer chemotherapeutic that inhibits both angiogenesis and the hedgehog (Hh) signaling pathway. We have synthesized and evaluated first and second generation ITZ analogues for their anti-Hh and anti-angiogenic activities to more fully probe the structural requirements for these anti-cancer properties. Our overall results suggest that the triazole functionality is required for ITZ-mediated inhibition of angiogenesis, but that it is not essential for inhibition of Hh signaling. The synthesis and evaluation of stereochemically defined *des*-triazole ITZ analogues also provides key information as to the optimal configuration around the dioxolane ring of the ITZ scaffold. Finally, the results from our studies suggest that two distinct cellular mechanisms of action govern the anti-cancer properties of the ITZ scaffold.

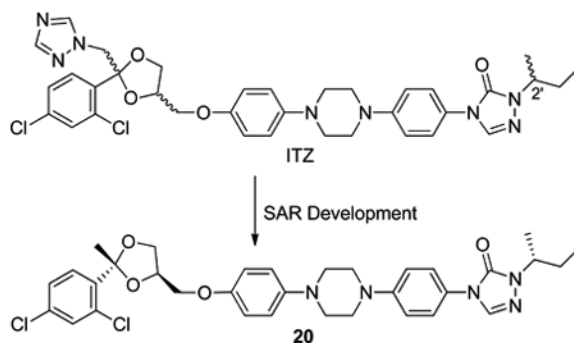
Graphical abstract

*To whom correspondence should be addressed. kyle.hadden@uconn.edu Phone: 1-860-486-8446. Fax: 1-860-486-6857.

[‡]These authors contributed equally to this work.

Supporting Information. Synthetic protocols and characterization of previously disclosed ITZ intermediates; ¹H and ¹³C NMR spectra for all new intermediates and final ITZ analogues; HSQC, NOESY, and x-ray crystal structures for select intermediates and final analogues.

Author Contributions: J.R.P. and A.M.D. synthesized ITZ analogues and performed biological evaluations. VS., S.K.T.-G., K.A.C., R.A.T., and D.S.R. performed biological assays. The manuscript was written through contributions of all authors. All authors have given approval to the final version of the manuscript.



Introduction

Identifying novel biological activities of FDA-approved drugs has emerged as a viable strategy to expedite the drug discovery process. The pharmacokinetic and toxicological profiles of these compounds are well-understood and they are inherently “drug-like.” To this end, drug development researchers have made a concerted effort to incorporate small molecule libraries containing approved drugs in their high-throughput screens. Recently, two such screens designed to repurpose FDA-approved compounds as anti-cancer chemotherapeutics identified itraconazole (ITZ) as both an inhibitor of the hedgehog (Hh) signaling pathway ($IC_{50} = 690$ nM) and angiogenesis ($IC_{50} = 160$ nM).¹⁻² ITZ is a clinically efficacious member of the 1,2,4-triazole class of anti-fungal agents that exerts its antimycotic effects through potent inhibition of lanosterol 14 α -demethylase (14LDM, also known as CYP51), a cytochrome P450 enzyme that catalyzes the oxidative conversion of lanosterol to ergosterol.³

The Hh pathway is a signaling cascade responsible for cell proliferation, differentiation, and tissue growth in embryogenesis.⁴⁻⁵ In healthy adults, the Hh pathway is considered less active and its primary role is maintaining stem cells in the skin and neural systems. Dysregulation of the Hh pathway, through a variety of different mechanisms, can lead to its constitutive activation, uncontrolled cellular proliferation, and tumor growth. Aberrant Hh pathway activation has been identified in a variety of cancers; however, the two most commonly identified as Hh-dependent are basal cell carcinoma (BCC) and medulloblastoma (MB).⁶⁻⁸ Because a significant portion of both BCCs (70%) and MBs (25%) rely on Hh signaling for tumorigenesis, it has drawn considerable interest for the development of targeted anti-cancer agents.⁹⁻¹⁰

The importance of angiogenesis in tumor formation, growth, and metastasis is well-documented and numerous small molecules and biologics that inhibit angiogenesis are clinically useful anti-cancer agents.¹¹⁻¹³ These angiogenesis inhibitors are primarily utilized to indirectly arrest tumor growth by inhibiting the growth of blood vessels and depriving tumor cells of oxygen and nutrients. In certain cases, combination therapy including a traditional first-line chemotherapy and an anti-angiogenic agent has demonstrated improved efficacy when compared to the chemotherapy alone.¹⁴ In addition, while most chemotherapeutic agents are toxic and confer resistance, anti-angiogenic agents have only shown mild side effects and there are no reported incidents of resistance.¹⁵⁻¹⁶

Although ITZ is clinically efficacious, several of its overall features are not inherently “drug-like”. The molecular weight of ITZ (706 g/mol) is above the threshold typically targeted for small molecule therapeutics (500 g/mol). Multiple formulations of ITZ have been developed and evaluated to improve its oral bioavailability and overall pharmacokinetic profile.¹⁷⁻¹⁸ In addition, the triazole moiety of ITZ has the ability to coordinate with the heme of CYP450s; most notably, CYP3A4, and ITZ-mediated inhibition of CYP3A4 is responsible for multiple drug-drug interactions and adverse side effects.¹⁹ If ITZ is to be used as a chemotherapeutic, drug-drug interactions need to be minimized as cancer patients are often taking multiple medications to both treat the cancer and manage symptoms. Herein we report the synthesis and evaluation of an extensive series of itraconazole analogues designed to probe the scaffold for the identification of functionalities required for its anti-Hh and anti-angiogenic properties.

Results

Analogue Design

As noted above, the triazole moiety of ITZ is both required for its anti-fungal properties and responsible for its main detrimental side effect, inhibition of CYP3A4. The N4 of the ITZ triazole interacts with the heme group in CYP51 and CYP3A4 to prevent coordination of the molecular oxygen required to initiate oxidation.²⁰⁻²¹ In addition to the triazole containing dioxolane region of the ITZ scaffold, ITZ contains a central phenyl-piperazine-phenyl linker region and a triazolone/side chain region (Chart 1). Within the context of its anti-fungal activity, the extended linker and triazolone/side chain regions are not essential for binding the active site of CYP51; however, they do interact with several amino acid residues in the substrate access channel.²² ITZ contains three chiral centers (2, 4, and 2') and can potentially exist as a mixture of eight distinct stereoisomers; however, formation of the *cis*-configurations around the dioxolane ring predominates during its synthesis and pharmaceutical preparations of ITZ are typically administered as a 1:1:1:1 mixture of the *cis* diastereomers.²³

To date, the only structural component of ITZ explored for Hh inhibition is the side chain region.²⁴ These side chain derivatives, as well as a series of stereochemically defined ITZ analogues, have been explored for their anti-angiogenic properties;²⁴⁻²⁵ however, an in-depth exploration of the structural requirements of the ITZ scaffold for these anti-cancer properties has not been undertaken. We have prepared and evaluated a first generation series of ITZ analogues that systematically truncates the scaffold from both the left- and right-hand side to identify key structural features required for inhibition of both Hh signaling and angiogenesis (Table 1).

Evaluation of this first generation series provided key structure-activity relationship (SAR) data that was subsequently utilized for the design of a second generation of stereochemically defined ITZ derivatives based on analogue **2** (Table 2). The second generation series was designed to determine whether a specific stereoisomer of key ITZ analogue **2** was responsible for its anti-Hh and/or anti-angiogenic properties.

Chemistry

Analogues **1-25** were synthesized following slightly modified literature procedures. All of these analogues contain the phenyl-piperazine-phenyl linker region of ITZ, which is initially constructed by a coupling step between commercially available N-(4-methoxyphenyl)-piperazine **26** and 1-chloro-4-nitrobenzene **27** to yield N-(4-hydroxyphenyl)-N'-(4-nitrophenyl)-piperazine **28** (Scheme 1). The nitro moiety in **28** is reduced to the aniline **29** in the presence of hydrazine monohydrate and 10% palladium on charcoal.²⁵ The aniline undergoes a series of well-characterized transformations to ultimately provide the key triazolone intermediate **32**. The methoxy substituent in starting material **26** serves as a protecting group throughout Scheme 1 and while other literature sources protect this phenol with a methoxymethyl (MOM) group, we found the synthetic scheme utilizing the MOM protection to be significantly less efficient in generating the corresponding key intermediate.²⁴

Triazolone **32** was alkylated with either commercially available alkyl bromides (**37-38**) or alkyl brosylates (**35-36**), which were prepared from the corresponding commercially available and stereochemically defined alcohols (**33-34**) (Scheme 2).²⁵ The methoxy group in the linker/triazolone/side chain intermediates (**39-42**) was removed with 48% hydrobromic acid in toluene to afford the phenols **43-46**.²⁶ It is important to note that alkylation of the triazolone results in an inversion of stereochemistry for the defined side chains; for example, (*R*)-brosylate **35** generates (*S*)-intermediates **39** and **43**.

The dioxolane regions were obtained via two different mechanisms due to their structural differences. Dioxolane regions that contained the triazole moiety could not be directly formed under standard ketalization procedures due to the basicity of the triazole functionality. For these intermediates, the triazole moiety (**50**) was added to various halogenated ketones (**47-49**) to form the triazole containing ketones (**51-53**). In parallel, tosylated glycerol **56** was formed through standard tosylation of the commercially available dioxolane **54** and subsequent acid-mediated hydrolysis (Scheme 3). Final dioxolane region intermediates containing the triazole moiety (**57-59**) were prepared through ketalization of **51-53** and **56** with triflic acid.

The *des*-triazole dioxolane regions (**61a-c** and **64-67**) were synthesized under standard ketalization reaction conditions utilizing a Dean-Stark apparatus (Scheme 4).²⁷ Stereochemically defined tosylated glycerols **62** and **63** were prepared via the method described above for the racemic mixture and each of the protected glycerols was used to ketalize 2,4-dichloroacetophenone.²⁵ For the stereochemically defined dioxolanes, the *cis*-isomer was predominantly formed (~3:1 *cis:trans*) and the isomers were easily separable via column chromatography.

Tosylated dioxolane regions were coupled with the linker/triazolone/side chain region phenols in anhydrous dimethyl sulfoxide with cesium carbonate to yield the final analogues **1-8** and **12-25** (Scheme 5A). The truncated triazolone analogues (**10-11**) were synthesized in reverse order.²⁵ The unprotected linker region **68**²⁴ was prepared in the same manner as **28** in Scheme 1 (Scheme 5B). This linker region intermediate was then coupled with the tosylated dioxolane region **59** under similar conditions described above to afford truncated

analogue **10**, which was reduced to the aniline with palladium on charcoal (10%) in the presence of hydrazine monohydrate to afford ITZ analogue **11**.²⁴ Overall purification methods varied for each ITZ analogue, particularly amongst the first generation series that contained the triazole moiety. Purification methods for all compounds are listed in the experimental or supplemental information.

Biological Evaluation

The initial evaluation of first generation ITZ analogues (**1-11**) as Hh pathway inhibitors was performed by monitoring endogenous Gli1 mRNA levels in C3H10T1/2 cells, an Hh-dependent mouse embryonic fibroblast (MEF) at a single concentration (1 μ M). In this well-studied model system for evaluating small molecule inhibition of Hh signaling, addition of an exogenous Hh agonist (recombinant Hh ligand or small molecule) results in a characteristic increase in Gli1 mRNA expression.²⁸ Concomitant incubation with a pathway inhibitor reduces Gli1 expression. Analogues that reduced Gli1 mRNA levels below 20% in this assay were subsequently evaluated for their ability to reduce Gli1 mRNA expression levels in a concentration-dependent fashion in these cells and the Hh-dependent murine BCC cell line ASZ.³⁰⁻³¹ In addition, several compounds were evaluated for their anti-proliferative effects in primary Hh-dependent medulloblastoma cells isolated from conditional patched knockout (*Math1-Cre-ER;Ptc^{fl/fl}*, MERP) mice.³²⁻³⁴ Based on the primary nature of the MERP cells, only a small subset of 1st and 2nd generation ITZ analogues were chosen for evaluation in these cells. Finally, each of these analogues was evaluated for its ability to inhibit proliferation in human umbilical vein epithelial cells (HUVECs). In vivo angiogenesis is dependent on endothelial cell proliferation; therefore, the inhibition of HUVEC proliferation is commonly utilized as an early stage in vitro model of anti-angiogenic activity.²⁴⁻²⁵ In addition, the identification of ITZ as an anti-angiogenic compound was established via this assay.² The results for these assays are given in Table 3.

Evaluation of the first generation of ITZ analogues indicated several structural features that appear necessary for Hh pathway inhibition. While the absolute stereochemistry at the 2'-position of the *sec*-butyl side chain does not appear important, **6** and **7** are equipotent in the MEF and ASZ cell lines, removing the methyl moiety (**8**) significantly reduces the overall activity of the scaffold. Interestingly, removing the side chain (**9**) or the triazolone/side chain (**10-11**) did not affect the Hh inhibitory activity of the scaffold as each of these analogues also demonstrated potent inhibition of pathway signaling in each cell line with IC₅₀ levels comparable to ITZ. In regards to modifications to the dioxolane region, removal of the chlorine atoms on the phenyl ring had minimal effects (**3**), while complete truncation of the phenyl ring (**4**) resulted in a significant loss of anti-Hh activity. Removal of the triazole moiety (**2**) had no effect on the ability of the scaffold to inhibit Hh signaling. Not surprisingly, removal of both the triazole and phenyl ring (**5**) or complete truncation to the phenol (**45**), significantly reduced Hh inhibitory activity. Our synthesized ITZ (**1**) demonstrated comparable activity to the ITZ purchased commercially in each of the cell lines evaluated. Finally, while each of the analogues evaluated was equipotent in its ability to down-regulate Gli1 mRNA expression in both the C3H10T1/2 and ASZ cells (Table 3), the ability of ITZ, **1**, and **11** to inhibit the proliferation of Hh-dependent murine MB cells was slightly reduced.

In addition to exploring Hh pathway inhibition, this first generation of ITZ analogues was evaluated for their ability to inhibit VEGF-induced proliferation in HUVECs, an initial step towards determining their ability to inhibit angiogenesis. The ITZ synthesized in the lab (**1**) demonstrated anti-proliferative activity comparable to the commercially purchased ITZ (GI_{50} values = 0.49 and 0.40 μ M, respectively). The remaining ITZ analogues were significantly less active than ITZ in this assay. Several analogues were moderately active (GI_{50} values, 1.7-8.4 μ M), but none were comparable to ITZ. Finally, we compared ITZ and **2** for their ability to inhibit CYP3A4. Not surprisingly, removal of the triazole moiety completely abolished the ability of **2** to inhibit CYP3A4 (IC_{50} values = 50.4 nM and >10 μ M, respectively, Supplementary Figure 1).

As noted above, the synthetic route primarily utilized to access ITZ results in a 1:1:1:1 ratio of four stereoisomers that share the *cis* configuration for the triazole and ether linker around the dioxolane ring. As a means to optimize our time and efforts related to the synthesis and evaluation of our first generation series of ITZ analogues, we did not fully characterize the ratio of stereoisomers present in each of the analogues. Instead they were evaluated as the stereoisomeric mixtures produced via the synthetic route(s) described. In order to more fully probe the absolute structural requirements of the scaffold for potent inhibition of Hh signaling and angiogenesis, we synthesized and evaluated a second generation series of stereochemically defined ITZ analogues based on the *des*-triazole ITZ analogue **2**. It is important to note that the nomenclature of the stereochemistry regarding the dioxolane region differs between ITZ and *des*-triazole ITZ analogues. The triazole moiety receives priority within the fully intact ITZ dioxolane region; therefore, the *cis*-orientation is in reference to the triazole and ether linkage (Chart 2). By contrast, removal of the triazole shifts priority to the phenyl ring and a *cis-des*-triazole analogue has the opposite absolute configuration between the phenyl ring and ether linker as ITZ. In addition, coupling of the dioxolane region intermediates to the linker/side chain phenol results in the opposite nomenclature assignment for the final ITZ analogue, for example, final analogues that have the 4*R* stereochemistry were prepared from the (*S*) tosylate **62**.

Evaluation of our stereochemically defined analogues for their ability to inhibit Hh signaling in the C3H10T1/2 and ASZ cell lines provided both interesting and confounding results. Overall, the majority of the compounds evaluated (**12-25**, Table 4) were more active in the ASZ cells, with numerous analogues exhibiting 100- to 1000-fold improvement in activity in these cells when compared to the MEFs. Several analogues that were inactive in the C3H10T1/2 MEFs at concentrations up to 10 μ M (**15**, **24-25**) induced potent down-regulation of Gli1 (IC_{50} values = 0.55, 0.2, and 0.54 μ M, respectively). In addition, several other compounds with modest inhibitory effects in the MEF cell line (**13**, **17**, and **21**) exhibited low nanomolar IC_{50} values in the ASZ cells.

Even with the conflicting results between cell lines, several interesting SAR developments with respect to optimal configuration were identified for our second generation ITZ analogues. First, these results reiterated that the orientation of the methyl moiety in the *sec*-butyl side chain is less important, as long as it is present (Table 4). Compounds that included a propyl moiety were significantly less active than analogues maintaining the same orientation around the dioxolane ring (i.e. **17** and **23**; **18** and **24**) and incorporating the *sec*-

butyl moiety. ITZ analogues with the *trans*-orientation around the dioxolane generally demonstrated enhanced down-regulation of Gli1 mRNA expression in both cell lines when compared to the corresponding *cis* analogues. Finally, compounds containing the 4*R* configuration were generally more active than corresponding analogues with the 4*S* configuration and *des*-triazole analogues with the *trans* 2*R*,4*R* configuration (**16**, **20**, and **22**) demonstrated the most comparable activity between the two cell lines.

Based on the anti-Hh activity of the stereochemically defined compounds in the C3H10T1/2 and ASZ cells, we evaluated several of these ITZ analogues in the primary MB cell line. The specific analogues selected for the anti-proliferative studies were chosen either because they were potent in both cell lines (**12** and **20**) or because they were significantly less active in the MEFs (**13**, **17**, **21**, **24**). Measuring the anti-proliferative effects of these analogues in the Hh-dependent primary cell culture would not only provide additional in vitro data for the most active *trans* analogues, but might also serve to clarify the discrepancies in anti-Hh activity between the two immortalized cell lines. Not surprisingly, the mixtures of *trans*- (**12**) and *cis*- (**13**) stereoisomers were less active than the single stereochemically defined analogues. The most active analogue in this assay was **17** (GI₅₀ = 0.39 μM), which has the *cis* 2*R*,4*R* configuration around the dioxolane moiety. Finally, the reduced anti-proliferative activity demonstrated for analogue **24** further highlights the importance of the methyl group on the side chain for Hh inhibition. Based on the anti-proliferative results in the MB cells, we chose to evaluate ITZ and three analogues (**17**, **20**, and **21**) for their ability to down-regulate endogenous Gli1 mRNA expression in the MERP MB cell line. Along with ITZ, each of these compounds exhibited potent down-regulation of mRNA expression in this assay further demonstrating their ability to inhibit Hh signaling (Table 5). It is important to note that the anti-Hh activity of the ITZ analogues in the MERP MB cells more closely correlated with the data obtained in the ASZ cells, suggesting that the immortalized BCC cell line may be a more appropriate early stage in vitro cellular model of Hh signaling for evaluating analogues based on the ITZ scaffold.

Following the initial identification of ITZ as an Hh pathway inhibitor, several additionalazole anti-fungals were evaluated for their anti-Hh properties.¹ Interestingly, the closely related, stereochemically defined triazole anti-fungal posaconazole (PSZ, Chart 2) was not explored in these early studies. Based on our findings that ITZ analogue **20** was the most consistent in its ability to inhibit pathway activity across multiple Hh-dependent cell lines, we also evaluated PSZ, which shares the same orientation around its tetrahydrofuran (THF) ring, in each of these assays. PSZ demonstrated potent down-regulation of Gli1 expression in the MEF and ASZ cell lines; however, it was significantly less active in the MERP cells. Taken together, these data strongly suggesting that the dioxolane and hydrophobic side chain of ITZ are more active than the corresponding THF and hydroxylated side chains of PSZ.

The second generation of ITZ analogues was also evaluated in the HUVECs for their anti-angiogenic activity. In a fashion similar to our initial series, each analogue evaluated in this assay was significantly less active than the commercially purchased ITZ. Interestingly, the *trans*- (**12**) and *cis*- (**13**) dioxolane mixtures were both more potent than the complete mixture (**2**). Our results did not yield a clear SAR pattern that distinguished one stereo-defined dioxolane region to be more potent against HUVEC anti-proliferation. The

stereoisomer that had the lowest IC₅₀, **17**, contains the (*R*)-*cis*-dioxolane region and the (*S*)-*sec*-butyl group (IC₅₀ = 2.5 ± 0.7 μM). When only the stereochemistry of the *sec*-butyl moiety is inverted (**21**), activity is attenuated (IC₅₀ = 12.8 ± 2.9 μM). Overall, the (*S*)-*sec*-butyl analogues have lower IC₅₀ values than the corresponding (*R*)-*sec*-butyl analogues. The same trend held true for the (*R*)-*trans*-dioxolane analogues (**16** and **20**); this was the most potent orientation determined from the Hh pathway evaluation. These results differ from the Hh pathway inhibitory activity of the scaffold in that the stereochemistry of the side chain region did not play a significant role in achieving potent inhibition. Taken together, there is not one dioxolane region that can be readily determined as the most potent across the second generation of ITZ analogues for inhibiting proliferation of HUVEC cells.

Based on the lack of clear SAR in the HUVEC cells, we sought to further explore the anti-angiogenic properties of ITZ and our analogues by evaluating their ability to inhibit tube formation in HUVECs grown on Matrigel. Under normal conditions, HUVECs plated and grown on Matrigel migrate towards each other, align, and form tubes that resemble in vivo capillary beds. This assay is generally considered a more robust model of angiogenesis as it requires several aspects of proper vessel formation, including adhesion, migration, and tube formation.²⁹ As tube formation assays are inherently lower-throughput, we chose to evaluate only a few select compounds, including, ITZ, **2**, **18**, **21**, and the well-characterized angiogenesis inhibitor suramin (positive control). These analogues were chosen for evaluation based on both their activity in the anti-proliferation assays and their overall structure in an attempt to provide the most relevant preliminary information with respect to the ability of this scaffold to inhibit angiogenesis.

Inhibition of tube formation (as measured by overall tube length and total tube junctions) by ITZ and **2** were comparable to that of the positive control suramin at 10 μM; however, neither of the stereochemically defined analogues (**18** and **21**) were active at this concentration (Figures 1 and 2). ITZ also demonstrated significant inhibition of tube formation at 1 μM. A decrease in activity was observed at 1 μM for analogue **2**, highlighting the importance of the triazole moiety for optimal anti-angiogenic activity of the scaffold. Interestingly, there was minimal correlation between the ability of a compound to inhibit anti-proliferation and tube formation in the HUVEC cells. ITZ was most active in both assay systems; however, analogues **18** and **21** were two-fold more active in the anti-proliferation assay than **2**, yet they were essentially inactive in the tube formation assay. Taken together, these data suggest that the triazole of ITZ is important for the anti-angiogenic activity of the scaffold and further SAR with respect to this region and its anti-cancer properties is warranted.

Discussion and Conclusions

The identification of two distinct anti-cancer activities for the FDA approved drug ITZ prompted our exploration of the structural characteristics of this scaffold that govern these activities. Based on previously published SAR for the side chain region of the ITZ scaffold,²⁴ it was not surprising that our preliminary data suggests no correlation between the anti-Hh and anti-angiogenic activity of these scaffolds. Significant modifications to multiple regions of the scaffold resulted in compounds that retained the ability to inhibit Hh

Smo) may be more responsive to the stereochemically defined analogues in the ASZ cells. In addition, Hh signaling in the C3H10T1/2 cells must be activated through the addition of an exogenous agonist (for these assays, recombinant sonic Hh ligand), while Hh signaling and Gli1 overexpression are constitutively active in the ASZ cells due to a heterozygous mutation in the *PTCH1* allele.³⁰⁻³¹ Up-regulation of pathway signaling with the Hh ligand in the MEFs may result in a level of Gli1 overexpression that cannot be fully overcome by the ITZ analogue(s). Finally, complete inhibition of Hh signaling for the ITZ scaffold may rely on the presence of multiple stereoisomers to fully inhibit its target, which could explain why the isomeric mixtures in the first generation demonstrated comparable activity across both cell lines. These discrepancies are currently being addressed in ongoing studies to more fully understand the mechanisms that govern ITZ-mediated inhibition of both cell lines.

A consideration for the further development of these and other ITZ analogues as potential Smo antagonists is that multiple forms of mutant Smo have been identified in both BCC and MB patients receiving a small molecule Smo antagonists.³⁶⁻⁴⁰ These mutations in Smo oftentimes render patients insensitive to further treatment with the Smo antagonists that have been approved by the FDA. A key rationale for developing ITZ analogues as Hh pathway inhibitors is that ITZ has previously demonstrated the ability to inhibit several resistant forms of Smo in vitro and in vivo;^{1,41} however, any further development of these analogues as Hh inhibitors must demonstrate that they also prevent pathway signaling in the presence of mutant Smo. Attempts to circumvent mutant Smo by developing small molecule Hh pathway inhibitors that function downstream of Smo at the level of the Gli transcription factors has emerged as a potential strategy to circumvent mutant Smo; however, all of the Gli inhibitors reported to date demonstrate only modest inhibition of Hh signaling, suggesting more studies are necessary to determine whether directly targeting Gli(s) is a valid therapeutic strategy.⁴²

In conclusion, we have synthesized and evaluated two series of ITZ analogues for their ability to inhibit both Hh signaling and angiogenesis. These studies have provided preliminary insight into the structural features required for potent inhibition of both of these cancer related pathways. Ongoing studies for the ITZ scaffold include further SAR exploration of the side chain and dioxolane region as well as studies designed to more fully understand the discrepancies in Hh inhibition demonstrated across the different Hh-dependent cell lines.

Experimental Section

Chemical Synthesis

General Information—Starting materials were purchased from Sigma-Aldrich or Fisher Scientific. ACS grade methanol, ethyl acetate, toluene, anhydrous DMF, NMP, and DMSO were purchased from Fisher Scientific or Sigma-Aldrich. ITZ analogue **9** was purchased from Toronto Research Chemicals. All reactions were run under an argon atmosphere. NMR data was collected on a Bruker AVANCE 500 MHz spectrometer and analysis performed using MestReNova. HRMS data was analyzed at the Mass Spectrometry Facility at the University of Connecticut by Dr. You-Jun Fu. FT-IR analysis was performed on a Bruker Alpha Platinum ATR instrument using OPUS software (v 7.2). The preparation of previously

characterized ITZ intermediates followed known procedures with minor modifications.^{24-26,32} X-ray crystals were prepared using vapor diffusion techniques (pentanes:chloroform) and analysis performed by Dr. Victor Day at the Small-Molecule X-ray Crystallography Lab at the University of Kansas on a Bruker MicroStar microfocussing Cu rotating anode generator with two CCD detectors or a Bruker Apex II CCD detector equipped with Helios multilayer optics instruments. Mercury (v3.0) software was used to visualize X-ray structural analysis. All ITZ analogues evaluated in the biological assays (**1-25**) were greater than 95% pure based on the HPLC methods described below.

Purity Analysis of Final Analogues—It is important to note that final ITZ analogues **1-11** were synthesized and evaluated as stereoisomeric mixtures. For this initial series, we did not separate individual stereoisomers nor did we determine the ratios of *cis:trans* dioxolanes produced in the ketalization reaction. These mixtures are reflected in the ¹H and ¹³C NMR characterization data described below and the spectra provided in the supplementary information. Purity analysis for all final analogues was determined via one of the methods described below.

Method A—ITZ analogues were dissolved in HPLC grade MeCN and injected (20 µl of a 1 mM soln) into an Agilent Manual FL-Injection Valve (600 bar) on an Agilent 1100/1200 Series HPLC equipped with an Agilent Eclipse Plus C18 (4.6 × 100 mm) column and Agilent 1100 Series Photodiode Array Detector. The mobile phase consisted of 60% MeCN:40% H₂O for analogues containing the triazole moiety and 70% MeCN:30% H₂O for *des*-triazole analogues. All analogues were run at a flow rate of 1.0 mL/min for 20 mins and purity was assessed at 254 nm.

Method B—ITZ analogues were dissolved in HPLC grade MeCN and injected (20 µl of a 1 mM soln) into an Agilent HPLC system coupled to an Agilent ESI single quadrupole mass spectrometer equipped with a Kinetix C18 (150 × 4.6 mm) column and an Agilent G1315 diode array detector. The mobile phase consisted of 70% MeCN:30% H₂O. All analogues were run at a flow rate of 0.7 mL/min for 30 mins and purity was assessed at 254 nm.

Previously Characterized ITZ Intermediates—Common ITZ linker region (**28-32** and **68**), dioxolane region (**53-56**, **59**, **62-63**), side chain (**35-36**), and coupled intermediates were prepared primarily as described previously for the ITZ scaffold with the minor modifications described in the supplementary info.^{24-26,35} Procedures and characterization for newly reported key intermediates and all final analogues is provided below.

First Generation ITZ Intermediates and Final Analogues (1-11)

1-(1*H*-1,2,4-triazol-1-yl)propan-2-one (51)—A solution of chloroacetone (**47**) (1.72 mL, 21.6 mmol), 1*H*-1,2,4-triazole (**50**) (2.98 g, 43.2 mmol), NaHCO₃ (2.89 g, 34.5 mmol), and toluene (100 mL) were heated to reflux (110-120°C) for 3 h. The reaction vessel was cooled to -20°C for 12 h. The resulting precipitate was filtered, dissolved in H₂O, and extracted with EtOAc (50 mL × 3). The organic layer was collected, washed with saturated sodium chloride (100 mL), and dried (Na₂SO₄). The solvent was evaporated and the crude product was purified via column chromatography (SiO₂, 0 - 3% MeOH in DCM) resulting in

a yellow oil (600 mg, 22.2%). ^1H NMR (500 MHz, CDCl_3) δ 8.01 (s, 1H), 7.76 (s, 1H), 4.90 (s, 2H), 2.00 (s, 3H). ^{13}C NMR (126 MHz, CDCl_3) δ 199.58, 151.41, 144.15, 57.52, 26.63. DART-HRMS: m/z calcd. for $\text{C}_5\text{H}_7\text{N}_3\text{O}$ $[\text{MH}]^+$, 126.0667; Found: 126.0691. IR (solid) ν_{max} : 3122, 2935, 2241, 1728, 1507, 1352, 1273, 1137, 1115, 727, 677, 646.

1-phenyl-2-(1H-1,2,4-triazol-1-yl)ethanone (52)—A solution of 2-bromoacetophenone (**48**) (2.0 g, 10.0 mmol), 1H-1,2,4-triazole (**50**) (1.4 g, 20.1 mmol), NaHCO_3 (1.3 g, 16.1 mmol), and toluene (100 mL) were heated to reflux (110-120°C) for 3 h. The reaction vessel was cooled to -20°C for 12 h. The resulting precipitate was filtered, dissolved in H_2O , and extracted with EtOAc (3 \times 50 mL). The organic layer was collected, washed with saturated sodium chloride, and dried over sodium sulfate. The solvent was evaporated and the crude product was purified via column chromatography (SiO_2 , 0 - 3% MeOH in DCM) resulting in a yellow solid (1.2 g, 64.1%). ^1H NMR (500 MHz, CDCl_3) δ 8.28 (s, 1H), 8.04 (s, 3H), 7.70 (s, 1H), 7.57 (s, 2H), 5.71 (s, 2H). ^{13}C NMR (126 MHz, CDCl_3) δ 190.84, 152.02, 145.07, 134.69, 129.30, 128.25, 55.19. DART-HRMS: m/z calcd. for $\text{C}_{10}\text{H}_9\text{N}_3\text{O}$ $[\text{MH}]^+$, 188.0824; Found: 188.0822. IR (solid) ν_{max} : 3113, 3062, 2992, 2953, 1697, 1596, 1504, 1450, 1345, 1225, 1207, 1135, 1021, 888, 752, 687, 675, 656, 634.

(2-((1H-1,2,4-triazol-1-yl) methyl)-2-methyl-1,3-dioxolan-4-yl) methyl 4-methylbenzenesulfonate (57)—Ketone **51** (1.4 g, 11.9 mmol) and **56** (2.8 g, 11.5 mmol) were added to a dry round bottom flask. Anhydrous toluene (10 mL) was added and the mixture was cooled to 0°C at which time TfOH (4.0 mL, 45.9 mmol) was added dropwise with a glass syringe. The solution was stirred at RT for 60 h. The mixture was diluted with 50 mL of EtOAc and slowly added to a solution of K_2CO_3 (5 g) in water (40 mL). The aqueous layer was washed with EtOAc (3 \times 50 mL) and the organic layers were combined, dried (Na_2SO_4), filtered, and concentrated. The crude product was purified via column chromatography (SiO_2 , 0 - 10% MeOH in DCM) (200 mg, <10%). ^1H NMR (500 MHz, CDCl_3) δ 8.10 (d, J = 8.3 Hz, 1H), 7.86 (s, 1H), 7.81 - 7.75 (m, 2H), 7.37 (m, 2H), 4.39 - 4.24 (m, 3H), 4.06 (m, 1H), 4.03 - 3.92 (m, 1H), 3.86 (m, 1H), 3.83 - 3.74 (m, 1H), 3.69 (m, 1H), 3.53 (m, 1H), 2.46 (d, J = 5.7 Hz, 3H), 1.32 (d, J = 5.9 Hz, 3H). ^{13}C NMR (126 MHz, CDCl_3) δ 152.04, 151.89, 145.75, 144.96, 132.89, 130.45, 130.39, 128.40, 74.56, 74.07, 68.83, 68.68, 67.17, 67.03, 55.93, 55.88, 23.77, 22.66, 22.09. DART-HRMS: m/z calcd. for $\text{C}_{15}\text{H}_{19}\text{N}_3\text{O}_5\text{S}$ $[\text{MH}]^+$, 354.1124; Found: 354.1124. IR (solid) ν_{max} : 3007, 2989, 2916, 2894, 1594, 1557, 1359, 1172, 1093, 1035, 961, 873, 724, 662, 563.

(2-((1H-1,2,4-triazol-1-yl)methyl)-2-phenyl-1,3-dioxolan-4-yl)methyl 4-methylbenzenesulfonate (58)—Crude dioxolane **58** was prepared through a procedure analogous to that described above for **57**. Following extraction with EtOAc, the combined organic layers were dried (Na_2SO_4), filtered, and concentrated to ~70 mL EtOAc. A solution of TsOH monohydrate (2.0 g) in EtOAc (13 mL) was slowly added at RT. The product precipitated as a salt and was filtered (3.9 g). The salt was dissolved in aqueous saturated K_2CO_3 (100 mL) and washed with DCM (3 \times 100 mL). The organic layers were combined, dried (Na_2SO_4) and used without further purification (62%). ^1H NMR (500 MHz, CDCl_3) δ 8.02 (s, 1H), 7.77 - 7.70 (m, 3H), 7.40 - 7.27 (m, 8H), 4.42 (d, J = 1.4 Hz, 2H), 4.22 - 4.13 (m, 1H), 3.75 (m, 2H), 3.61 (m, 1H), 3.47 (m, 1H), 2.42 (s, 3H). ^{13}C NMR (126 MHz,

CDCl₃) δ 151.12, 145.23, 138.05, 132.33, 129.98, 129.27, 128.62, 127.94, 125.64, 108.44, 73.42, 68.52, 66.55, 55.71, 21.65. DART-HRMS: *m/z* calcd. for C₂₀H₂₁N₃O₅S [MH]⁺, 416.1280; Found: 416.1263. IR (solid) ν_{max}: 3311, 3111, 2992, 2953, 2893, 1596, 1509, 1448, 1349, 1336, 1232, 1172, 1043, 968, 811, 736, 699, 611, 551.

(2-(2,4-dichlorophenyl)-2-methyl-1,3-dioxolan-4-yl)methyl 4-methylbenzenesulfonate (61a)—To a solution of 2',4'-dichloroacetophenone (**60**) (20 g, 0.1 mol) in toluene (80 mL) was added glycerol (11 g, 0.12 mol) followed by a catalytic amount of *p*-toluenesulfonic acid monohydrate (475 mg, 2.5 mmol). A Dean-Stark trap (10 mL trap filled with 8 mL toluene) and condenser were fitted atop the reaction flask. The solution was refluxed for 48 h. Upon cooling, the mixture was diluted with EtOAc and washed sequentially with saturated sodium bicarbonate (3 × 100 mL), water (2 × 100 mL), and saturated sodium chloride (100 mL). The organic layer was dried (MgSO₄), filtered, concentrated, and purified by column chromatography (SiO₂, 3:1 Hex: EtOAc) to yield **61a** as a clear oil in excellent yield (88%). ¹H NMR (500 MHz, CDCl₃) δ 7.78 (d, *J* = 8.2 Hz, 1H), 7.47 (m, 1H), 7.36 – 7.31 (m, 2H), 7.31 – 7.27 (m, 1H), 7.18 – 7.14 (m, 1H), 4.16 (m, 1H), 4.10 – 4.00 (m, 2H), 3.89 – 3.77 (m, 1H), 3.68 (m, 1H), 2.43 (s, 1H), 2.42 (s, 2H), 1.66 (d, *J* = 1.0 Hz, 3H). ¹³C NMR (126 MHz, CDCl₃) δ 144.98, 137.50, 134.44, 132.50, 130.95, 130.69, 129.80, 129.74, 128.58, 128.11, 127.81, 127.71, 126.64, 126.56, 109.26, 109.23, 73.62, 72.69, 69.32, 68.53, 66.32, 65.98, 25.46, 25.38, 21.48. DART-HRMS: *m/z* calcd. for C₁₈H₁₈Cl₂O₅S [MH]⁺, 417.0330; Found: 417.0306. IR (solid) ν_{max}: 2988, 2941, 2889, 1586, 1556, 1464, 1364, 1188, 1174, 1095, 1035, 979, 809, 662, 552.

4-(4-(4-(4-((2-((1H-1,2,4-triazol-1-yl)methyl)-2-(2,4-dichlorophenyl)-1,3-dioxolan-4-yl)methoxy)phenyl)piperazin-1-yl)phenyl)-2-(sec-butyl)-2,4-dihydro-3H-1,2,4-triazol-3-one (1)—To a solution of **45** (50 mg, 0.127 mol) in DMSO (2 mL) was added dioxolane tosylate **59** (67 mg, 0.139 mmol) followed by Cs₂CO₃ (0.41 mg, 1.27 mmol). The mixture was warmed to 80 °C and stirred for 16 h. The mixture was cooled to RT and water was added slowly (6 mL) with vigorous stirring to form a precipitate. The precipitate was filtered, washed with water, and determined to be the product with only DMOS as an impurity. The precipitate was dissolved in EtOAc (60 mL) and washed with water (50 mL). The aqueous layer was washed with EtOAc (1 × 50 mL) and the combined organic layers were dried (Na₂SO₄), filtered, and concentrated. The crude residue was purified by column chromatography (SiO₂, 0-80% acetone in hexanes) and sonicated in pentanes to produce **1** as a white solid (62 mg, 69%). ¹H NMR (500 MHz, CDCl₃) δ 8.20 (d, *J* = 8.2 Hz, 1H), 7.91 (d, *J* = 10.6 Hz, 1H), 7.64 – 7.55 (m, 2H), 7.50 – 7.39 (m, 3H), 7.06 – 6.99 (m, 2H), 6.94 (d, *J* = 9.1 Hz, 1H), 6.88 (d, *J* = 8.9 Hz, 1H), 6.84 – 6.77 (m, 1H), 6.69 – 6.61 (m, 1H), 4.88 – 4.70 (m, 2H), 4.40 – 4.19 (m, 2H), 3.96 – 3.87 (m, 1H), 3.85 – 3.76 (m, 2H), 3.54 – 3.44 (m, 1H), 3.36 (m, 4H), 3.23 (m, 4H), 1.87 (m, 1H), 1.72 (m, 1H), 1.39 (dd, *J* = 6.7, 1.4 Hz, 3H), 0.91 (m, 3H). ¹³C NMR (126 MHz, CDCl₃) δ 152.52, 152.43, 151.94, 151.49, 151.31, 150.45, 145.94, 145.89, 144.81, 144.60, 135.98, 135.70, 134.97, 133.97, 133.81, 133.04, 132.89, 131.35, 131.06, 129.52, 129.42, 127.15, 126.98, 125.87, 123.46, 118.37, 118.27, 116.58, 115.19, 115.08, 74.62, 67.57, 67.37, 54.30, 53.53, 52.58, 50.49, 49.15, 28.35, 19.17, 10.70. DART-HRMS: *m/z* calcd. for C₃₅H₃₈Cl₂N₈O₄ [MH]⁺, 705.2471; Found: 705.2474. IR (solid) ν_{max}: 3125, 2966, 2832,

1698, 1585, 1551, 1510, 1450, 1379, 1228, 1184, 1139, 1042, 976, 944, 824, 736. Purity: 98.0% (Method A).

1-(sec-butyl)-4-(4-(4-(4-((2-(2,4-dichlorophenyl)-2-methyl-1,3-dioxolan-4-yl)methoxy)phenyl)piperazin-1-yl)phenyl)-1H-1,2,4-triazol-5(4H)-one (2)—To a solution of **45** (64 mg, 0.163 mmol) in DMSO (10 mL) was added sodium hydride (1.14 mmol). The mixture was warmed to 50° C and stirred for 2 h. To this solution was added **61a** (62 mg, 0.148 mmol in DMSO, 5 mL). The solution was warmed to 90° C and stirred for 12 h. The mixture was cooled to RT and H₂O (30 mL) was added slowly with vigorous stirring. The mixture was washed with EtOAc (3 × 100 mL), and the organic layers were combined, dried (Na₂SO₄), filtered, and concentrated. The crude residue was purified by column chromatography (SiO₂, 0-5% MeOH in DCM) to afford **2** as a reddish-brown solid in modest yield (34%). A portion of **2** was dissolved in chloroform and slow evaporation provided off-white crystals that were utilized for the biological assays. ¹H NMR (500 MHz, CDCl₃) δ 7.66 – 7.59 (m, 2H), 7.46 – 7.36 (m, 3H), 7.21 (m, 1H), 7.06 – 7.00 (m, 2H), 7.01 – 6.71 (m, 4H), 4.37 – 4.25 (m, 2H), 4.12 (m, 1H), 4.01 (m, 1H), 3.96 (m, 1H), 3.79 (m, 1H), 3.36 (d, *J* = 6.2 Hz, 4H), 3.31 – 3.17 (m, 4H), 1.89 – 1.82 (m, 1H), 1.82 (s, 3H), 1.78 (s, 1H), 1.72 (m, 1H), 1.39 (d, *J* = 6.7 Hz, 3H), 0.90 (t, *J* = 7.4 Hz, 3H). ¹³C NMR (126 MHz, CDCl₃) δ 152.0, 150.5, 138.1, 134.5, 133.8, 132.8, 131.1, 128.8, 128.5, 126.7, 126.6, 125.9, 123.5, 118.4, 116.6, 115.5, 109.0, 73.9, 69.2, 66.9, 52.7, 50.6, 49.2, 28.4, 25.8, 25.7, 19.2, 10.7. DART-HRMS: *m/z* calcd. for C₃₃H₃₈Cl₂N₅O₄ [MH]⁺, 638.2301; Found: 638.2298. IR (solid) ν_{max} 2960, 2922, 2874, 2850, 1696, 1552, 1509, 1462, 1449, 1376, 1226, 1192, 1149, 1076, 1034, 870, 734. Purity: 98.0% (Method A).

4-(4-(4-(4-((1H-1,2,4-triazol-1-yl)methyl)-2-phenyl-1,3-dioxolan-4-yl)methoxy)phenyl)piperazin-1-yl)phenyl)-1-(sec-butyl)-1H-1,2,4-triazol-5(4H)-one (3)—ITZ analogue **3** was prepared using the general method described above for analogue **1** utilizing the requisite linker/side chain and dioxolane intermediates (23 mg, 47%). ¹H NMR (500 MHz, CDCl₃) δ 8.20 (s, 1H), 7.91 (s, 1H), 7.61 (s, 1H), 7.57 – 7.51 (m, 2H), 7.46 – 7.34 (m, 5H), 7.06 – 7.00 (m, 2H), 6.96 – 6.90 (m, 2H), 6.82 – 6.76 (m, 2H), 4.54 (d, *J* = 1.6 Hz, 2H), 4.39 – 4.25 (m, 2H), 3.90 (dd, *J* = 8.4, 6.7 Hz, 1H), 3.77 (m, 2H), 3.44 (m, 1H), 3.39 – 3.33 (m, 4H), 3.26 – 3.16 (m, 4H), 1.93 – 1.80 (m, 1H), 1.78 – 1.65 (m, 1H), 1.39 (d, *J* = 6.8 Hz, 3H), 0.90 (t, *J* = 7.4 Hz, 3H). ¹³C NMR (126 MHz, CDCl₃) δ 152.45, 151.61, 145.20, 139.21, 134.33, 129.63, 129.08, 126.23, 123.97, 118.89, 117.09, 115.69, 74.96, 68.39, 67.73, 56.33, 53.09, 51.03, 49.65, 28.86, 19.67, 11.21. DART-HRMS: *m/z* calcd. for C₃₅H₄₀N₈O₄ [MH]⁺, 637.3251; Found: 637.3271. IR (solid) ν_{max} 3122, 3058, 2961, 2825, 1693, 1602, 1551, 1508, 1448, 1388, 1327, 1296, 1226, 1180, 1135, 1939, 944, 823, 736, 701, 676. Purity: 97.1% (Method A).

4-(4-(4-(4-((1H-1,2,4-triazol-1-yl)methyl)-2-methyl-1,3-dioxolan-4-yl)methoxy)phenyl)piperazin-1-yl)phenyl)-2-(sec-butyl)-2,4-dihydro-3H-1,2,4-triazol-3-one (4)—ITZ analogue **4** was prepared using the general method described above for analogue **1** utilizing the requisite linker/side chain and dioxolane intermediates. (45%) ¹H NMR (500 MHz, CDCl₃) δ 8.30 – 8.10 (m, 1H), 7.94 (s, 1H), 7.62 (s, 1H), 7.43 (d, *J* = 8.5 Hz, 2H), 7.03 (d, *J* = 8.9 Hz, 2H), 6.97 – 6.87 (m, 2H), 6.84 (t, *J* = 9.9 Hz, 2H),

4.49 (t, $J = 5.8$ Hz, 1H), 4.39 (s, 1H), 4.36 – 4.24 (m, 2H), 4.15 (m, 1H), 4.03 – 3.84 (m, 1H), 3.79 (m, 1H), 3.69 – 3.59 (m, 1H), 3.42 – 3.33 (m, 4H), 3.24 (t, $J = 5.0$ Hz, 4H), 1.92 – 1.81 (m, 1H), 1.72 (m, 1H), 1.44 (s, 1H), 1.43 – 1.36 (m, 5H), 0.90 (t, $J = 7.4$ Hz, 3H). ^{13}C NMR (126 MHz, CDCl_3) δ 152.7, 152.0, 151.4, 150.5, 145.9, 144.6, 133.9, 125.9, 123.5, 118.5, 118.4, 116.6, 115.3, 115.2, 108.0, 75.4, 74.8, 68.5, 67.7, 67.5, 67.1, 55.7, 55.6, 52.6, 50.6, 49.2, 28.4, 23.5, 22.5, 19.2, 10.7. IR (solid) ν_{max} 3121, 3053, 2930, 2850, 2809, 1702, 1683, 1548, 1510, 1471, 1452, 1336, 1251, 1134, 1106, 1068, 1050, 940, 883, 735. DART-HRMS: m/z calcd. for $\text{C}_{30}\text{H}_{39}\text{N}_8\text{O}_4$ $[\text{MH}]^+$, 575.3094; Found: 575.3090. IR (solid) ν_{max} : 2967, 2934, 2878, 2837, 1701, 1554, 1510, 1450, 1382, 1225, 1181, 1136, 1042, 1017, 942, 826, 784. Purity: 95.1% (Method A).

1-(sec-butyl)-4-(4-(4-(4-((2,2-dimethyl-1,3-dioxolan-4-yl)methoxy)phenyl)piperazin-1-yl)phenyl)-1*H*-1,2,4-triazol-5(4*H*)-one (5)—ITZ analogue **5** was prepared using the general method described above for analogue **2** utilizing the requisite linker/side chain and dioxolane intermediates. The crude residue was purified via column chromatography (SiO_2 , 0-5% MeOH in DCM) to afford **5** in modest yield (14 mg, 21%) ^1H NMR (500 MHz, CDCl_3) δ 7.61 (d, $J = 7.2$ Hz, 1H), 7.43 (d, $J = 8.4$ Hz, 2H), 7.03 (d, $J = 8.5$ Hz, 2H), 6.94 (s, 1H), 6.89 (d, $J = 8.4$ Hz, 2H), 4.46 (m, 1H), 4.29 (m, 1H), 4.16 (t, $J = 7.4$ Hz, 1H), 4.04 (m, 1H), 3.90 (m, 2H), 3.37 (s, 2H), 3.24 (s, 2H), 1.86 (m, 1H), 1.71 (m, 1H), 1.46 (s, 3H), 1.39 (d, $J = 7.8$ Hz, 6H), 0.91 (t, $J = 7.4$ Hz, 3H). ^{13}C NMR (126 MHz, CDCl_3) δ 152.44, 134.28, 124.08, 123.96, 118.93, 117.14, 115.81, 110.13, 74.49, 69.77, 67.32, 53.11, 51.11, 49.62, 33.08, 28.86, 27.22, 25.79, 19.66, 11.20. DART-HRMS: m/z calcd. for $\text{C}_{28}\text{H}_{37}\text{N}_5\text{O}_4$ $[\text{MH}]^+$, 508.2924; Found: 508.2909. IR (solid) ν_{max} : 3126, 3060, 2967, 2926, 2878, 2828, 2212, 1681, 1584, 1556, 1510, 1452, 1380, 1226, 1149, 1037, 941, 819, 736. Purity: 97.5% (Method B).

4-(4-(4-(4-((1*H*-1,2,4-triazol-1-yl)methyl)-2-(2,4-dichlorophenyl)-1,3-dioxolan-4-yl)methoxy)phenyl)piperazin-1-yl)phenyl)-2-((*S*)-sec-butyl)-2,4-dihydro-3*H*-1,2,4-triazol-3-one (6)—ITZ analogue **6** was prepared using the general method described above for analogue **1** utilizing the requisite linker/side chain and dioxolane intermediates (55%). ^1H NMR (500 MHz, CDCl_3) δ 8.20 (s, 1H), 7.89 (s, 1H), 7.61 (s, 1H), 7.57 (d, $J = 8.3$ Hz, 1H), 7.47 (d, $J = 2.1$ Hz, 1H), 7.43 (d, $J = 8.9$ Hz, 2H), 7.03 (d, $J = 9.0$ Hz, 2H), 6.94 (m, 2H), 6.80 (m, 2H), 4.80 (m, 2H), 4.36 (m, 1H), 4.28 (m, 1H), 3.92 (m, 1H), 3.81 (m, 2H), 3.48 (m, 1H), 3.36 (m, 4H), 3.23 (m, 4H), 1.86 (m, 1H), 1.72 (m, 1H), 1.39 (d, $J = 6.7$ Hz, 3H), 0.90 (t, $J = 7.4$ Hz, 3H). ^{13}C NMR (126 MHz, CDCl_3) δ 152.6, 151.4, 150.5, 146.0, 144.8, 136.0, 134.0, 133.8, 133.1, 131.4, 129.6, 127.2, 125.9, 123.5, 118.4, 116.6, 115.2, 109.9, 107.6, 74.7, 67.6, 67.4, 53.6, 52.6, 50.5, 49.2, 28.4, 19.2, 10.7. DART-HRMS: m/z calcd. for $\text{C}_{35}\text{H}_{39}\text{Cl}_2\text{N}_8\text{O}_4$ $[\text{MH}]^+$, 705.2471; Found: 705.2465. IR (solid) ν_{max} : 2967, 2930, 2878, 1695, 1586, 1552, 1509, 1451, 1378, 1226, 1183, 1130, 1038, 947, 816, 736. Purity: 97.9% (Method A).

4-(4-(4-(4-((1*H*-1,2,4-triazol-1-yl)methyl)-2-(2,4-dichlorophenyl)-1,3-dioxolan-4-yl)methoxy)phenyl)piperazin-1-yl)phenyl)-2-((*R*)-sec-butyl)-2,4-dihydro-3*H*-1,2,4-triazol-3-one (7)—ITZ analogue **7** was prepared using the general method described above for analogue **1** utilizing the requisite linker/side chain and

dioxolane intermediates (77%). ¹H NMR (500 MHz, CDCl₃) δ 8.20 (s, 1H), 7.89 (s, 1H), 7.64 – 7.54 (m, 2H), 7.50 – 7.40 (m, 3H), 7.03 (d, *J* = 8.6 Hz, 2H), 6.95 (s, 1H), 6.81 (d, *J* = 8.4 Hz, 2H), 4.84 (d, *J* = 14.7 Hz, 1H), 4.76 (d, *J* = 14.7 Hz, 1H), 4.39 – 4.25 (m, 2H), 3.92 (m, 1H), 3.86 – 3.77 (m, 2H), 3.50 (m, 1H), 3.38 (s, 2H), 3.25 (s, 3H), 1.87 (m, 1H), 1.72 (m, 1H), 1.39 (d, *J* = 6.7 Hz, 3H), 0.91 (t, *J* = 7.4 Hz, 3H). ¹³C NMR (126 MHz, CDCl₃) δ 152.5, 152.0, 151.3, 150.5, 146.0, 136.0, 134.0, 133.8, 133.1, 131.4, 129.5, 127.2, 125.9, 123.5, 118.4, 116.6, 115.2, 107.6, 77.2, 74.7, 67.6, 67.4, 53.6, 52.6, 50.5, 49.2, 28.4, 19.2, 10.7. DART-HRMS: *m/z* calcd. for C₃₅H₃₉Cl₂N₈O₄ [MH]⁺, 705.2471; Found: 705.2468 IR (solid) ν_{max}: 3067, 2966, 2934, 2878, 2832, 1695, 1585, 1551, 1509, 1450, 1379, 1225, 1180, 1136, 1039, 944, 820, 794. Purity: 95.0% (Method A).

4-(4-(4-(4-((2-((1*H*-1,2,4-triazol-1-yl)methyl)-2-(2,4-dichlorophenyl)-1,3-dioxolan-4-yl)methoxy)phenyl)piperazin-1-yl)phenyl)-1-propyl-1*H*-1,2,4-triazol-5(4*H*)-one (8)—ITZ analogue **8** was prepared using the general method described above for analogue **2** utilizing the requisite linker/side chain and dioxolane intermediates (50 mg, 68%). ¹H NMR (500 MHz, CDCl₃) δ 8.20 (s, 1H), 7.89 (s, 1H), 7.59 (d, *J* = 21.6 Hz, 2H), 7.48 (s, 1H), 7.41 (s, 2H), 7.04 (s, 2H), 6.93 (s, 2H), 6.81 (s, 2H), 4.80 (d, *J* = 23.3 Hz, 2H), 4.36 (s, 1H), 3.92 (s, 1H), 3.82 (s, 4H), 3.52 (s, 1H), 3.37 (s, 4H), 3.24 (s, 5H), 1.84 (s, 2H), 0.98 (s, 3H). ¹³C NMR (126 MHz, CDCl₃) δ 152.60, 136.48, 134.30, 133.55, 131.85, 130.02, 127.65, 123.98, 117.08, 115.73, 108.05, 75.13, 68.11, 54.05, 51.01, 49.60, 47.62, 22.43, 11.50. DART-HRMS: *m/z* calcd. for C₃₄H₃₆Cl₂N₈O₄ [MH]⁺, 691.2315; Found: 691.2329. IR (solid) ν_{max}: 3068, 2960, 2925, 2873, 2835, 1696, 1585, 1553, 1510, 1452, 1379, 1225, 1160, 1136, 1045, 944, 823, 794. Purity: 95.2% (Method A).

1-(4-((2-((1*H*-1,2,4-triazol-1-yl)methyl)-2-(2,4-dichlorophenyl)-1,3-dioxolan-4-yl)methoxy)phenyl)-4-(4-nitrophenyl)piperazine (10)—To a solution of **68** (100 mg, 0.336 mmol) in DMSO (4 mL) was added Cs₂CO₃ (1.1 g, 3.36 mmol) and **59** (0.29 g, 0.604 mmol). The solution was warmed to 90° C and stirred for 12 h. The mixture was cooled to room temperature and water was added slowly with vigorous stirring (~6 mL). A yellow precipitate formed, which was filtered and recrystallized in EtOH to yield **10** (150 mg, 73%). ¹H NMR (500 MHz, CDCl₃) δ 8.22 – 8.12 (m, 3H), 7.90 (s, 1H), 7.58 (d, *J* = 8.5 Hz, 1H), 7.48 (d, *J* = 2.1 Hz, 1H), 6.95 – 6.86 (m, 4H), 6.86 – 6.78 (m, 2H), 4.84 (d, *J* = 14.8 Hz, 1H), 4.76 (d, *J* = 14.7 Hz, 1H), 4.36 (m, 1H), 3.92 (m, 1H), 3.85 – 3.75 (m, 3H), 3.61 – 3.55 (m, 4H), 3.48 (m, 1H), 3.26 – 3.20 (m, 4H). ¹³C NMR (126 MHz, CDCl₃) δ 154.79, 152.90, 151.42, 145.67, 144.94, 138.79, 136.14, 134.08, 133.17, 131.49, 129.63, 127.28, 125.99, 118.58, 115.39, 112.90, 107.69, 74.72, 67.71, 67.45, 53.63, 50.33, 47.29. DART-HRMS: *m/z* calcd. for C₂₉H₂₈Cl₂N₆O₅ [MH]⁺, 611.1577; Found: 611.1601. IR (solid) ν_{max}: 3116, 2923, 2852, 1589, 1557, 1506, 1456, 1377, 1318, 1226, 1136, 1029, 975, 942, 896, 823, 737, 691. Purity: 95.0% (Method A).

4-(4-(4-(4-((2-((1*H*-1,2,4-triazol-1-yl)methyl)-2-(2,4-dichlorophenyl)-1,3-dioxolan-4-yl)methoxy)phenyl)piperazin-1-yl)aniline (11)—10% palladium on carbon (1.04 mg, 5% mole ratio) was added to a dry round bottom flask. Ethanol (25 mL) was added followed by slow addition of **10** (120 mg, 0.196 mmol). Hydrazine monohydrate (0.06 mL, 1.96 mmol) was added dropwise and the mixture was stirred at reflux for 2 h. Upon cooling to

RT, the mixture was filtered through celite. The celite was washed with ethanol (100 mL) and chloroform (250 mL) to ensure complete elution of the aniline. The filtrate was concentrated to afford a yellow solid, which was recrystallized in EtOH to afford **11** (70 mg, 61%). ¹H NMR (500 MHz, CDCl₃) δ 8.20 (s, 1H), 8.15 (d, *J* = 9.4 Hz, 2H), 7.89 (s, 1H), 7.57 (d, *J* = 8.4 Hz, 1H), 7.47 (m, 1H), 7.25 (m, 1H), 6.92 (m, 2H), 6.88 (d, *J* = 9.5 Hz, 2H), 6.80 (d, *J* = 9.0 Hz, 2H), 4.80 (m, 2H), 4.36 (m, 1H), 3.91 (m, 1H), 3.80 (m, 2H), 3.58 (m, 4H), 3.47 (m, 1H), 3.22 (m, 4H). ¹³C NMR (126 MHz, CDCl₃) δ 154.7, 152.8, 151.3, 145.6, 144.9, 138.7, 136.1, 134.0, 133.1, 131.4, 129.6, 127.2, 125.9, 118.5, 115.3, 112.8, 107.6, 74.6, 67.6, 67.4, 53.6, 50.3, 47.2. DART-HRMS: *m/z* calcd. for C₂₉H₃₁Cl₂N₆O₃ [MH]⁺, 581.1835; Found: 581.1818. IR (solid) ν_{max}: 3084, 2886, 2827, 1558, 1504, 1313, 1224, 113, 1030, 942, 821, 749. Purity: 96.1% (Method A).

Second Generation ITZ Intermediates and Final Analogues (12-25)

(2-(2,4-dichlorophenyl)-2-methyl-1,3-dioxolan-4-yl)methyl 4-methylbenzenesulfonate (61b) and (2-(2,4-dichlorophenyl)-2-methyl-1,3-dioxolan-4-yl)methyl 4-methylbenzenesulfonate (61c)—The defined *trans* (**61b**) and *cis* (**61c**) mixtures of des-triazole dioxolane tosylates were prepared by extensive column chromatography (SiO₂, 0 - 20% EtOAc in Hex) on the complete mixture of tosylate stereoisomers **61a**. Fraction 1 (R_f ~ 0.7 in 3:1 Hex:EtOAc) was characterized as 2,4-anti-substituted dioxolanes (**61b**) and Fraction 2 (R_f ~ 0.6 in 3:1 Hex:EtOAc) was characterized as the 2,4-syn-substituted dioxolanes (**61c**) [Combined yield = 90%; Fraction 1 (**61b**) = 60%; Fraction 2 (**61c**) = 35%]. Fraction 1 crystallized over time whereas Fraction 2 remained a clear oil.

61b—¹H NMR (500 MHz, CDCl₃) δ 7.82 (d, *J* = 8.2 Hz, 2H), 7.49 (d, *J* = 8.3 Hz, 1H), 7.39 – 7.32 (m, 3H), 7.20 (m, 1H), 4.21 – 4.14 (m, 1H), 4.10 (m, 1H), 4.03 (m, 1H), 3.87 (m, 1H), 3.72 (m, 1H), 2.46 (s, 3H), 1.70 (s, 3H). ¹³C NMR (126 MHz, CDCl₃) δ 145.11, 137.59, 134.67, 132.69, 132.66, 131.17, 129.92, 128.67, 128.00, 126.78, 109.43, 72.80, 69.36, 66.22, 25.55, 21.65. DART-HRMS: *m/z* calcd. for C₁₈H₁₈Cl₂O₅S [MH]⁺, 417.0330; Found: 417.0345. IR (solid) ν_{max}: 3007, 2989, 2937, 2894, 1585, 1557, 1465, 1359, 1186, 1172, 1093, 1036, 811, 751, 663, 552, 492.

61c—¹H NMR (500 MHz, CDCl₃) δ 7.76 – 7.61 (m, 2H), 7.46 (d, *J* = 8.5 Hz, 1H), 7.36 – 7.29 (m, 3H), 7.11 (m, 1H), 4.52 – 4.38 (m, 1H), 4.20 (m, 1H), 3.92 (m, 1H), 3.80 (m, 1H), 3.57 (m, 1H), 2.47 (s, 3H), 1.70 (d, *J* = 1.1 Hz, 3H). ¹³C NMR (126 MHz, CDCl₃) δ 145.10, 138.65, 134.45, 132.59, 132.38, 130.92, 129.87, 128.21, 127.90, 126.72, 109.48, 73.73, 68.57, 66.60, 25.63, 21.67. DART-HRMS: *m/z* calcd. for C₁₈H₁₈Cl₂O₅S [MH]⁺, 417.0330; Found: 417.0347. IR (solid) ν_{max}: 2988, 2939, 2888, 1586, 1556, 1464, 1364, 1188, 1174, 1095, 1034, 979, 808, 662, 522.

((2R,4S)-2-(2,4-dichlorophenyl)-2-methyl-1,3-dioxolan-4-yl)methyl 4-methylbenzenesulfonate (64) and ((2S,4S)-2-(2,4-dichlorophenyl)-2-methyl-1,3-dioxolan-4-yl)methyl 4-methylbenzenesulfonate (65)—Stereochemically-defined tosylated *des*-triazole intermediates **64** and **65** were prepared from **60** and tosylated glycerol **62** using the general method described above for **61a**. Following initial column

chromatography, ~740 mg of the **64:65** mixture was loaded on a preparative TLC plate (Analtech Uniplate, 20 × 20 cm, 2000 mm coating thickness, Silica G). The plate was developed repeatedly (8× in 8:1 Hex:EtOAc). Following development and separation, the two bands were stripped from the TLC plate and the compounds removed from the silica beads by gentle stirring (5% MeOH in DCM, 200 mL, 12 h).

(64)—White solid, 45%. $R_f = 0.7$ in 3:1 Hex:EtOAc. $^1\text{H NMR}$ (500 MHz, CHCl_3) 7.78 (m, 3H), 7.48 (d, $J = 8.4$ Hz, 1H), 7.34 (m, 3H), 7.17 (m, 1H), 4.18 (m, 1H), 4.08 (m, 1H), 4.02 (m, 1H), 3.84 (m, 1H), 3.69 (m, 1H), 2.43 (s, 3H), 1.67 (s, 3H). $^{13}\text{C NMR}$ (126 MHz, CDCl_3) δ 145.0, 143.7, 138.9, 137.5, 134.5, 132.5, 132.5, 131.0, 129.8, 129.7, 129.7, 128.6, 127.8, 127.3, 126.6, 109.2, 72.7, 69.3, 66.0, 25.4, 21.5, 21.3. DART-HRMS: m/z calcd. for $\text{C}_{18}\text{H}_{18}\text{Cl}_2\text{O}_5\text{S}$ $[\text{MH}]^+$, 417.0330; Found: 417.0327. IR (solid) ν_{max} : 3093, 3007, 2989, 2916, 2894, 1585, 1556, 1359, 1186, 1172, 1093, 1035, 960, 940, 861, 751, 662, 551, 492.

(65)—Clear oil, 25%. $R_f = 0.6$ in 3:1 Hex:EtOAc. $^1\text{H NMR}$ (500 MHz, CHCl_3) 7.69 (d, $J = 8.2$ Hz, 2H), 7.46 (d, $J = 8.4$ Hz, 1H), 7.31 (m, 3H), 7.10 (m, 1H), 4.44 (m, 1H), 4.19 (m, 1H), 3.91 (m, 1H), 3.80 (m, 1H), 3.56 (m, 1H), 2.46 (s, 3H), 1.70 (s, 3H). $^{13}\text{C NMR}$ (126 MHz, CDCl_3) δ 145.0, 138.6, 134.4, 132.5, 132.3, 130.9, 129.8, 128.2, 127.8, 126.7, 109.4, 73.7, 68.5, 66.5, 29.6, 25.6, 21.6. DART-HRMS: m/z calcd. for $\text{C}_{18}\text{H}_{18}\text{Cl}_2\text{O}_5\text{S}$ $[\text{MH}]^+$, 417.0330; Found: 417.0325. IR (solid) ν_{max} : 3117, 3054, 2955, 2822, 1687, 1551, 1353, 1229, 1187, 1173, 1095, 1033, 967, 943, 824, 809, 663, 552, 531.

((2S,4R)-2-(2,4-dichlorophenyl)-2-methyl-1,3-dioxolan-4-yl)methyl 4-methylbenzenesulfonate (66) and ((2R,4R)-2-(2,4-dichlorophenyl)-2-methyl-1,3-dioxolan-4-yl)methyl 4-methylbenzenesulfonate (67)—Stereochemically-defined tosylated *des*-triazole intermediates **66** and **67** were prepared from **60** and tosylated glycerol **63** using the general method described above for **61a** and purified as described for **64** and **65**.

(66)—Crystalline, 55%. $R_f = 0.6$ in 3:1 Hex:EtOAc. $^1\text{H NMR}$ (500 MHz, CHCl_3) 7.81 (m, 3H), 7.49 (d, $J = 8.4$ Hz, 1H), 7.36 (m, 3H), 7.19 (m, 1H), 4.18 (m, 1H), 4.09 (m, 1H), 4.02 (m, 1H), 3.86 (m, 1H), 3.70 (m, 1H), 2.45 (s, 3H), 1.69 (s, 3H). $^{13}\text{C NMR}$ (126 MHz, CDCl_3) δ 145.1, 137.5, 134.6, 132.6, 132.6, 131.1, 129.9, 128.6, 127.9, 127.9, 126.7, 109.4, 72.7, 69.3, 66.1, 25.5, 21.6. DART-HRMS: m/z calcd. for $\text{C}_{18}\text{H}_{18}\text{Cl}_2\text{O}_5\text{S}$ $[\text{MH}]^+$, 417.0330; Found: 417.0358. IR (solid) ν_{max} : 3094, 3008, 2989, 2957, 2936, 2917, 2894, 1593, 1557, 1359, 1186, 1172, 1094, 1036, 961, 940, 862, 752, 662, 552, 493.

(67)—Clear oil, 30%. $R_f = 0.5$ in 3:1 Hex:EtOAc. $^1\text{H NMR}$ (500 MHz, CHCl_3) 7.69 (m, 2H), 7.46 (d, $J = 8.4$ Hz, 1H), 7.31 (m, 3H), 7.10 (m, 1H), 4.45 (m, 1H), 4.20 (m, 1H), 3.91 (m, 1H), 3.80 (m, 1H), 3.56 (m, 1H), 2.46 (s, 3H), 1.70 (s, 3H). $^{13}\text{C NMR}$ (126 MHz, CDCl_3) δ 145.1, 138.6, 134.4, 132.5, 132.3, 130.9, 129.8, 128.2, 127.9, 126.7, 109.4, 73.7, 68.5, 66.6, 25.6, 21.6. DART-HRMS: m/z calcd. for $\text{C}_{18}\text{H}_{18}\text{Cl}_2\text{O}_5\text{S}$ $[\text{MH}]^+$, 417.0330; Found: 417.0356. IR (solid) ν_{max} : 3094, 3007, 2989, 2957, 2917, 2894, 1585, 1557, 1358, 1185, 1172, 1093, 1036, 961, 939, 862, 751, 662, 551, 492.

General protocol for tosylate/phenol coupling and final analogue purification

—To a solution of alkyl-substituted phenol (**43-46**) (40 mg, 0.102 mmol) in DMSO (2.0 mL) was added *des*-triazole-tosylate (**61b-61c**, **64-67**) (46 mg, 0.110 mmol) followed by Cs₂CO₃ (0.82 mmol). The mixture was warmed to 80° C and stirred for 16 h. The mixture was then cooled to RT and water was added slowly (6 mL) with vigorous stirring, which resulted in formation of a precipitate. The mixture was transferred to a separatory funnel, diluted with EtOAc (60 mL) and washed with water (50 mL). The aqueous layer was washed with EtOAc (1 × 60 mL). The organic layers were combined, dried (MgSO₄), filtered, and concentrated. The crude residue was purified by column chromatography (SiO₂, 0 to 24% acetone in hexanes) to afford **2**, **12-25** as white to slightly off-white solids in good yields (45-88%). Final analogues were subsequently sonicated in pentanes (10-30 min) to remove a “grease-like” impurity (observed in ¹H NMRs at 0.88, 1.31 ppm) and collected for purity analysis and biological evaluation following filtration on a fine-fritted glass Buchner style filter funnel.

4-(4-(4-(4-((2-((1H-1,2,4-triazol-1-yl)methyl)-2-(2,4-dichlorophenyl)-1,3-dioxolan-4-yl)methoxy)phenyl)piperazin-1-yl)phenyl)-2-(sec-butyl)-2,4-dihydro-3H-1,2,4-triazol-3-one (12)—¹H NMR (500 MHz, CDCl₃) δ 7.62 (m, 2H), 7.42 (m, 3H), 7.23 (m, 1H), 7.03 (m, 2H), 6.92 (m, 2H), 4.31 (m, 2H), 4.11 (m, 1H), 4.01 (m, 1H), 3.97 (m, 1H), 3.84 (m, 1H), 3.36 (m, 4H), 3.24 (m, 4H), 1.87 (m, 1H), 1.81 (s, 3H), 1.72 (m, 1H), 1.39 (d, *J* = 6.7 Hz, 3H), 0.91 (t, *J* = 7.4 Hz, 3H). ¹³C NMR (126 MHz, CDCl₃) δ 152.7, 152.0, 150.5, 145.8, 139.2, 134.2, 133.8, 132.7, 130.9, 128.5, 126.6, 125.9, 123.5, 118.3, 116.6, 115.2, 109.1, 73.9, 69.3, 66.9, 52.6, 50.6, 49.2, 28.4, 25.6, 19.2, 10.7. DART-HRMS: *m/z* calcd. for C₃₃H₃₈Cl₂N₅O₄ [MH]⁺, 638.2301; Found: 638.2328. IR (solid) ν_{max} 2961, 2918, 2849, 1694, 1584, 1556, 1509, 1449, 1374, 1329, 1294, 1224, 1186, 1149, 1094, 1035, 1017, 942, 873, 821, 802, 734. Purity: 97.0% (Method B).

4-(4-(4-(4-((2-((1H-1,2,4-triazol-1-yl)methyl)-2-(2,4-dichlorophenyl)-1,3-dioxolan-4-yl)methoxy)phenyl)piperazin-1-yl)phenyl)-2-(sec-butyl)-2,4-dihydro-3H-1,2,4-triazol-3-one (13)—¹H NMR (500 MHz, CDCl₃) δ 7.63 (d, *J* = 8.5 Hz, 1H), 7.61 (s, 1H), 7.42 (m, 2H), 7.38 (d, *J* = 2.1 Hz, 1H), 7.19 (m, 1H), 7.01 (m, 2H), 6.89 (m, 2H), 6.73 (m, 2H), 4.60 (m, 1H), 4.29 (m, 2H), 3.94 (m, 1H), 3.73 (m, 1H), 3.35 (m, 4H), 3.21 (m, 4H), 1.85 (m, 1H), 1.77 (s, 3H), 1.71 (m, 1H), 1.39 (d, *J* = 6.7 Hz, 3H), 0.90 (t, *J* = 7.4 Hz, 3H). ¹³C NMR (126 MHz, CDCl₃) δ 152.7, 152.0, 150.5, 145.8, 139.2, 134.2, 133.8, 132.7, 130.9, 128.5, 126.6, 125.9, 123.5, 118.3, 116.6, 115.2, 109.1, 75.0, 68.3, 67.3, 52.6, 50.5, 49.2, 28.4, 25.8, 19.2, 10.7. HRMS: *m/z* calcd. for C₃₃H₃₈Cl₂N₅O₄ [MH]⁺, 638.2301; Found: 638.2325. IR (solid) ν_{max} 3102, 3008, 2961, 2918, 2899, 2849, 1699, 1597, 1538, 1515, 1411, 1355, 1337, 1254, 1236, 1189, 1159, 1106, 1064, 1036, 1024, 999, 936, 896, 831, 807, 741. Purity: 95.1% (Method B).

2-((S)-sec-butyl)-4-(4-(4-(4-(((2S,4S)-2-(2,4-dichlorophenyl)-2-methyl-1,3-dioxolan-4-yl)methoxy)phenyl)piperazin-1-yl)phenyl)-2,4-dihydro-3H-1,2,4-triazol-3-one (14)—¹H NMR (500 MHz, CDCl₃) δ 7.61 (m, 3H), 7.42 (m, 2H), 7.40 (m, 1H), 7.23 (m, 1H), 7.02 (m, 2H), 6.94 (m, 2H), 6.88 (m, 2H), 4.31 (m, 2H), 4.11 (m, 1H), 4.00 (m, 1H), 3.96 (m, 1H), 3.36 (m, 4H), 3.23 (m, 4H), 1.85 (m, 1H), 1.81 (s, 3H), 1.72 (m,

1H), 1.39 (d, $J = 6.7$ Hz, 3H), 0.91 (t, $J = 7.4$ Hz, 3H). ^{13}C NMR (126 MHz, CDCl_3) δ 152.9, 152.0, 150.5, 145.9, 138.1, 134.5, 133.8, 132.8, 131.1, 128.8, 126.7, 125.9, 123.5, 118.4, 116.6, 115.4, 109.0, 73.9, 69.2, 66.9, 52.6, 50.6, 49.2, 28.4, 25.7, 19.2, 10.7. DART-HRMS: m/z calcd. for $\text{C}_{33}\text{H}_{38}\text{Cl}_2\text{N}_5\text{O}_4$ $[\text{MH}]^+$, 638.2301; Found: 638.2282. IR (solid) ν_{max} 2962, 2875, 2826, 1694, 1555, 1509, 1448, 1374, 1224, 1186, 1149, 1035, 942, 824, 735. Purity: 97.4% (Method A).

2-((S)-sec-butyl)-4-(4-(4-(4-(((2R,4S)-2-(2,4-dichlorophenyl)-2-methyl-1,3-dioxolan-4-yl)methoxy)phenyl)piperazin-1-yl)phenyl)-2,4-dihydro-3H-1,2,4-triazol-3-one (15)— ^1H NMR (500 MHz, CDCl_3) δ 7.64 (d, $J = 8.4$ Hz, 2H), 7.61 (s, 1H), 7.42 (d, $J = 8.5$ Hz, 2H), 7.38 (d, $J = 2.2$ Hz, 2H), 7.19 (m, 1H), 7.02 (d, $J = 8.5$ Hz, 2H), 6.90 (d, $J = 8.5$ Hz, 2H), 6.73 (d, $J = 8.5$ Hz, 2H), 4.60 (m, 1H), 4.30 (m, 2H), 3.94 (m, 1H), 3.73 (m, 2H), 3.35 (m, 4H), 3.21 (m, 4H), 1.86 (m, 1H), 1.78 (s, 3H), 1.72 (m, 1H), 1.39 (d, $J = 6.7$ Hz, 3H), 0.91 (t, $J = 7.4$ Hz, 3H). ^{13}C NMR (126 MHz, CDCl_3) δ 152.8, 152.0, 150.5, 145.8, 139.3, 134.3, 133.8, 132.7, 130.9, 128.5, 126.6, 125.9, 123.5, 118.4, 116.6, 115.2, 109.1, 75.0, 68.4, 67.3, 52.6, 50.6, 49.2, 28.4, 25.8, 19.2, 10.7. DART-HRMS: m/z calcd. for $\text{C}_{33}\text{H}_{38}\text{Cl}_2\text{N}_5\text{O}_4$ $[\text{MH}]^+$, 638.2301; Found: 638.2288. IR (solid) ν_{max} 2923, 2851, 1714, 1703, 1683, 1613, 1548, 1509, 1452, 1374, 1271, 1226, 1188, 1150, 1094, 1035, 965, 942, 817, 735. Purity: 95.5% (Method A).

2-((S)-sec-butyl)-4-(4-(4-(4-(((2R,4R)-2-(2,4-dichlorophenyl)-2-methyl-1,3-dioxolan-4-yl)methoxy)phenyl)piperazin-1-yl)phenyl)-2,4-dihydro-3H-1,2,4-triazol-3-one (16)— ^1H NMR (500 MHz, CDCl_3) δ 7.61 (m, 2H), 7.41 (m, 3H), 7.23 (m, 1H), 7.02 (m, 2H), 6.94 (m, 2H), 6.89 (m, 2H), 4.31 (m, 2H), 4.11 (m, 1H), 4.00 (m, 1H), 3.96 (m, 1H), 3.84 (m, 1H), 3.36 (m, 4H), 3.23 (m, 4H), 1.86 (m, 1H), 1.81 (s, 3H), 1.72 (m, 1H), 1.39 (d, $J = 6.7$ Hz, 3H), 0.91 (t, $J = 7.4$ Hz, 3H). ^{13}C NMR (126 MHz, CDCl_3) δ 152.9, 152.0, 150.5, 145.9, 138.1, 134.5, 133.8, 132.8, 131.1, 128.8, 126.7, 125.9, 123.5, 118.4, 116.6, 115.4, 109.0, 73.9, 69.2, 66.9, 52.6, 50.6, 49.2, 28.4, 25.7, 19.2, 10.7. DART-HRMS: m/z calcd. for $\text{C}_{33}\text{H}_{38}\text{Cl}_2\text{N}_5\text{O}_4$ $[\text{MH}]^+$, 638.2301; Found: 638.2284. IR (solid) ν_{max} 2966, 2935, 2874, 2824, 1693, 1584, 1555, 1508, 1464, 1447, 1373, 1293, 1223, 1186, 1149, 1095, 1035, 942, 875, 824, 734. Purity: 97.3% (Method A).

2-((S)-sec-butyl)-4-(4-(4-(4-(((2S,4R)-2-(2,4-dichlorophenyl)-2-methyl-1,3-dioxolan-4-yl)methoxy)phenyl)piperazin-1-yl)phenyl)-2,4-dihydro-3H-1,2,4-triazol-3-one (17)— ^1H NMR (500 MHz, CDCl_3) δ 7.64 (d, $J = 8.5$ Hz, 1H), 7.61 (s, 1H), 7.42 (m, 2H), 7.38 (d, $J = 2.1$ Hz, 1H), 7.19 (m, 1H), 7.02 (m, 2H), 6.89 (m, 2H), 6.73 (m, 2H), 4.60 (m, 1H), 4.30 (m, 2H), 3.94 (m, 1H), 3.73 (m, 2H), 3.35 (m, 4H), 3.21 (m, 4H), 1.85 (m, 1H), 1.78 (s, 3H), 1.72 (m, 1H), 1.39 (d, $J = 6.7$ Hz, 3H), 0.91 (t, $J = 7.4$ Hz, 3H). ^{13}C NMR (126 MHz, CDCl_3) δ 152.8, 152.0, 150.5, 145.8, 139.3, 134.3, 133.8, 132.7, 130.9, 128.5, 126.6, 125.9, 123.5, 118.4, 118.4, 116.6, 115.2, 109.1, 75.0, 68.4, 67.3, 52.6, 50.6, 49.2, 28.4, 25.8, 19.2, 10.7. DART-HRMS: m/z calcd. for $\text{C}_{33}\text{H}_{38}\text{Cl}_2\text{N}_5\text{O}_4$ $[\text{MH}]^+$, 638.2301; Found: 638.2281. IR (solid) ν_{max} 2919, 2876, 2849, 1693, 1585, 1555, 1509, 1450, 1375, 1329, 1295, 1225, 1188, 1149, 1095, 1034, 934, 872, 819, 734. Purity: 98.4% (Method A).

2-((*R*)-sec-butyl)-4-(4-(4-(4-(((2*S*,4*S*)-2-(2,4-dichlorophenyl)-2-methyl-1,3-dioxolan-4-yl)methoxy)phenyl)piperazin-1-yl)phenyl)-2,4-dihydro-3*H*-1,2,4-triazol-3-one (18)—¹H NMR (500 MHz, CDCl₃) δ 7.61 (m, 2H), 7.42 (m, 2H), 7.41 (m, 1H), 7.23 (m, 1H), 7.03 (m, 2H), 6.94 (m, 2H), 6.89 (m, 2H), 4.31 (m, 2H), 4.11 (m, 1H), 4.01 (m, 1H), 3.96 (m, 1H), 3.84 (m, 1H), 3.36 (m, 4H), 3.23 (m, 4H), 1.87 (m, 1H), 1.81 (s, 3H), 1.72 (m, 1H), 1.39 (d, *J* = 6.7 Hz, 3H), 0.91 (t, *J* = 7.4 Hz, 3H). ¹³C NMR (126 MHz, CDCl₃) δ 152.9, 152.0, 150.5, 145.9, 138.1, 134.5, 133.8, 132.8, 131.1, 128.8, 126.7, 125.9, 123.5, 118.4, 116.6, 115.4, 109.0, 73.9, 69.2, 66.9, 52.6, 50.6, 49.2, 28.4, 25.7, 19.2, 10.7. DART-HRMS: *m/z* calcd. for C₃₃H₃₈Cl₂N₅O₄ [MH]⁺, 638.2301; Found: 638.2282. IR (solid) ν_{max} 2967, 2932, 2878, 2827, 1695, 1612, 1586, 1552, 1510, 1460, 1377, 1292, 1253, 1225, 1187, 1147, 1096, 1036, 940, 827, 735. Purity: 95.0% (Method B).

2-((*R*)-sec-butyl)-4-(4-(4-(4-(((2*R*,4*S*)-2-(2,4-dichlorophenyl)-2-methyl-1,3-dioxolan-4-yl)methoxy)phenyl)piperazin-1-yl)phenyl)-2,4-dihydro-3*H*-1,2,4-triazol-3-one (19)—¹H NMR (500 MHz, CDCl₃) δ 7.64 (d, *J* = 8.5 Hz, 1H), 7.61 (s, 1H), 7.42 (m, 2H), 7.38 (m, 1H), 7.20 (m, 1H), 7.02 (m, 2H), 6.90 (m, 2H), 6.73 (m, 2H), 4.60 (m, 1H), 4.30 (m, 1H), 3.94 (m, 1H), 3.73 (m, 1H), 3.35 (m, 4H), 3.21 (m, 4H), 1.86 (m, 1H), 1.78 (s, 3H), 1.71 (m, 1H), 1.39 (d, *J* = 6.7 Hz, 3H), 0.91 (t, *J* = 7.4 Hz, 3H). ¹³C NMR (126 MHz, CDCl₃) δ 152.9, 152.0, 150.5, 145.9, 138.1, 134.5, 133.8, 132.8, 131.1, 128.7, 126.7, 125.9, 123.5, 118.4, 116.6, 115.4, 109.0, 73.9, 69.2, 66.9, 52.6, 50.6, 49.2, 28.4, 25.7, 19.2, 10.7. DART-HRMS: *m/z* calcd. for C₃₃H₃₈Cl₂N₅O₄ [MH]⁺, 638.2301; Found: 638.2287. IR (solid) ν_{max} 3060, 2967, 2932, 2830, 1698, 1611, 1586, 1550, 1512, 1461, 1384, 1296, 1252, 1225, 1189, 1149, 1098, 1036, 940, 896, 824, 735. Purity: 95.0% (Method B).

2-((*R*)-sec-butyl)-4-(4-(4-(4-(((2*R*,4*R*)-2-(2,4-dichlorophenyl)-2-methyl-1,3-dioxolan-4-yl)methoxy)phenyl)piperazin-1-yl)phenyl)-2,4-dihydro-3*H*-1,2,4-triazol-3-one (20)—¹H NMR (500 MHz, CDCl₃) δ 7.61 (m, 2H), 7.43 (m, 2H), 7.41 (m, 1H), 7.23 (m, 1H), 7.03 (m, 2H), 6.94 (m, 2H), 6.89 (m, 2H), 4.31 (m, 2H), 4.11 (m, 1H), 4.01 (m, 1H), 3.96 (m, 1H), 3.84 (m, 1H), 3.36 (m, 4H), 3.23 (m, 4H), 1.86 (m, 1H), 1.81 (s, 3H), 1.72 (m, 1H), 1.39 (d, *J* = 6.7 Hz, 3H), 0.91 (t, *J* = 7.4 Hz, 3H). ¹³C NMR (126 MHz, CDCl₃) δ 153.0, 152.0, 150.5, 145.9, 138.1, 134.5, 133.8, 132.8, 131.1, 128.8, 126.7, 125.9, 123.5, 118.4, 116.6, 115.4, 109.0, 73.9, 69.2, 67.0, 52.6, 50.6, 49.2, 28.4, 25.7, 19.2, 10.7. DART-HRMS: *m/z* calcd. for C₃₃H₃₈Cl₂N₅O₄ [MH]⁺, 638.2301; Found: 638.2285. IR (solid) ν_{max} 2971, 2937, 2879, 2827, 1697, 1509, 1451, 1376, 1296, 1225, 1194, 1147, 1073, 1035, 942, 819, 734. Purity: 97.5% (Method B).

2-((*R*)-sec-butyl)-4-(4-(4-(4-(((2*S*,4*R*)-2-(2,4-dichlorophenyl)-2-methyl-1,3-dioxolan-4-yl)methoxy)phenyl)piperazin-1-yl)phenyl)-2,4-dihydro-3*H*-1,2,4-triazol-3-one (21)—¹H NMR (500 MHz, CDCl₃) δ 7.64 (d, *J* = 8.5 Hz, 2H), 7.61 (s, 1H), 7.42 (m, 2H), 7.37 (m, 1H), 7.19 (m, 1H), 7.02 (m, 2H), 6.90 (m, 2H), 6.73 (m, 2H), 4.60 (m, 1H), 4.30 (m, 2H), 3.95 (m, 1H), 3.73 (m, 2H), 3.35 (m, 4H), 3.22 (m, 4H), 1.86 (m, 1H), 1.78 (s, 3H), 1.72 (m, 1H), 1.39 (d, *J* = 6.7 Hz, 3H), 0.91 (t, *J* = 7.4 Hz, 3H). ¹³C NMR (126 MHz, CDCl₃) δ 152.8, 152.0, 150.5, 145.9, 139.3, 134.3, 133.8, 132.7, 130.9, 128.5, 126.6, 125.9, 123.5, 118.4, 118.4, 116.6, 115.2, 109.1, 75.0, 68.4, 67.3, 52.6, 50.6, 49.2, 28.4, 25.8,

19.2, 10.7. DART-HRMS: m/z calcd. for $C_{33}H_{38}Cl_2N_5O_4$ $[MH]^+$, 638.2301; Found: 638.2284. IR (solid) ν_{max} 2966, 2932, 2904, 2829, 1695, 1553, 1512, 1460, 1444, 1399, 1382, 1254, 1224, 1187, 1148, 1063, 1036, 939, 827, 735. Purity: 96.4% (Method A).

4-(4-(4-(4-(((2*R*,4*R*)-2-(2,4-dichlorophenyl)-2-methyl-1,3-dioxolan-4-yl)methoxy)phenyl)piperazin-1-yl)phenyl)-2-propyl-2,4-dihydro-3*H*-1,2,4-triazol-3-one (22)— 1H NMR (500 MHz, $CDCl_3$) δ 7.61 (m, 2H), 7.41 (m, 3H), 7.23 (m, 1H), 7.02 (m, 2H), 6.94 (m, 2H), 6.89 (m, 2H), 4.32 (m, 1H), 4.11 (m, 1H), 4.01 (m, 1H), 3.96 (m, 1H), 3.82 (m, 3H), 3.36 (m, 4H), 3.23 (m, 4H), 1.84 (m, 2H), 1.81 (s, 3H), 0.98 (t, $J = 7.4$ Hz, 3H). ^{13}C NMR (126 MHz, $CDCl_3$) δ 153.0, 152.1, 150.6, 145.9, 138.1, 134.5, 133.8, 132.8, 131.1, 128.8, 126.7, 125.8, 123.5, 118.4, 116.6, 115.4, 109.0, 73.9, 69.2, 66.9, 50.6, 49.2, 47.2, 25.7, 22.0, 11.1. DART-HRMS: m/z calcd. for $C_{32}H_{36}Cl_2N_5O_4$ $[MH]^+$, 624.2144; Found: 624.2143. IR (solid) ν_{max} 3125, 3059, 2935, 2876, 2829, 1703, 1686, 1614, 1585, 1551, 1510, 1454, 1405, 1375, 1336, 1297, 1225, 1194, 1143, 1094, 1035, 944, 869, 814, 733. Purity: 96.6% (Method B).

4-(4-(4-(4-(((2*SV*,4*R*)-2-(2,4-dichlorophenyl)-2-methyl-1,3-dioxolan-4-yl)methoxy)phenyl)piperazin-1-yl)phenyl)-2-propyl-2,4-dihydro-3*H*-1,2,4-triazol-3-one (23)**— 1H NMR (500 MHz, $CDCl_3$) δ 7.64 (d, $J = 8.4$ Hz, 1H), 7.60 (s, 1H), 7.41 (m, 2H), 7.38 (d, $J = 2.1$ Hz, 1H), 7.20 (m, 1H), 7.02 (d, $J = 8.9$ Hz, 2H), 6.90 (d, $J = 8.9$ Hz, 2H), 6.73 (d, $J = 8.9$ Hz, 2H), 4.64 (m, 1H), 4.30 (m, 1H), 3.94 (m, 1H), 3.82 (t, $J = 7.2$ Hz, 2H), 3.73 (m, 2H), 3.35 (m, 4H), 3.21 (m, 4H), 1.83 (m, 2H), 1.78 (s, 3H), 0.98 (t, $J = 7.4$ Hz, 3H). ^{13}C NMR (126 MHz, $CDCl_3$) δ 152.8, 152.1, 150.5, 145.8, 139.3, 134.3, 133.8, 132.7, 130.9, 128.5, 126.6, 125.8, 123.5, 118.4, 116.6, 115.2, 109.1, 99.9, 75.0, 68.3, 67.3, 50.6, 49.2, 47.2, 25.8, 22.0, 11.1. HRMS: m/z calcd. for $C_{32}H_{36}Cl_2N_5O_4$ $[MH]^+$, 624.2144; Found: 624.2142. IR (solid) ν_{max} 2966, 2932, 2904, 2830, 1698, 1609, 1585, 1550, 1511, 1461, 1402, 1385, 1336, 1296, 1224, 1189, 1148, 1097, 1036, 940, 875, 824, 735. Purity: 96.5% (Method B).

4-(4-(4-(4-(((2*SV*,4*S**V*)-2-(2,4-dichlorophenyl)-2-methyl-1,3-dioxolan-4-yl)methoxy)phenyl)piperazin-1-yl)phenyl)-2-propyl-2,4-dihydro-3*H*-1,2,4-triazol-3-one (24)**— 1H NMR (500 MHz, $CDCl_3$) δ 7.64 (d, $J = 8.4$ Hz, 1H), 7.60 (s, 1H), 7.41 (d, $J = 8.8$ Hz, 2H), 7.38 (d, $J = 2.1$ Hz, 1H), 7.02 (m, 2H), 6.90 (d, $J = 8.5$ Hz, 2H), 6.73 (m, 2H), 4.60 (m, 1H), 4.30 (m, 1H), 3.94 (m, 1H), 3.81 (t, $J = 7.2$ Hz, 2H), 3.73 (m, 2H), 3.35 (m, 4H), 3.22 (m, 4H), 1.83 (m, 2H), 1.78 (s, 3H), 0.98 (t, $J = 7.4$ Hz, 3H). ^{13}C NMR (126 MHz, $CDCl_3$) δ 153.0, 152.1, 150.6, 145.9, 138.1, 134.5, 133.8, 132.8, 131.1, 128.8, 126.7, 125.8, 123.5, 118.4, 116.6, 115.4, 109.0, 73.9, 69.2, 66.9, 50.6, 49.2, 47.2, 25.7, 22.0, 11.1. DART-HRMS: m/z calcd. for $C_{32}H_{36}Cl_2N_5O_4$ $[MH]^+$, 624.2144; Found: 624.2140. IR (solid) ν_{max} 2919, 2876, 2849, 1693, 1601, 1585, 1555, 1509, 1450, 1403, 1375, 1331, 1295, 1225, 1188, 1149, 1095, 1032, 1017, 943, 871, 814, 734. Purity: 95.4% (Method B).

4-(4-(4-(4-(((2*R*,4*SV*)-2-(2,4-dichlorophenyl)-2-methyl-1,3-dioxolan-4-yl)methoxy)phenyl)piperazin-1-yl)phenyl)-2-propyl-2,4-dihydro-3*H*-1,2,4-triazol-3-one (25)**— 1H NMR (500 MHz, $CDCl_3$) δ 7.61 (m, 2H), 7.41 (m, 3H), 7.23 (m,

1H), 7.03 (m, 2H), 6.95 (m, 2H), 6.89 (m, 2H), 4.32 (m, 1H), 4.11 (m, 1H), 4.00 (m, 1H), 3.94 (m, 1H), 3.82 (m, 3H), 3.37 (m, 4H), 3.24 (m, 4H), 1.83 (m, 2H), 1.81 (s, 3H), 0.98 (t, $J = 7.4$ Hz, 3H). ^{13}C NMR (126 MHz, CDCl_3) δ 153.0, 152.1, 150.5, 145.9, 138.0, 134.5, 133.8, 132.7, 131.1, 128.8, 126.7, 125.9, 123.5, 118.4, 116.6, 115.4, 109.0, 73.9, 69.2, 66.9, 50.6, 49.1, 47.2, 25.7, 22.0, 11.0. DART-HRMS: m/z calcd. for $\text{C}_{32}\text{H}_{36}\text{Cl}_2\text{N}_5\text{O}_4$ $[\text{MH}]^+$, 624.2144; Found: 624.2105. IR (solid) ν_{max} 2918, 2876, 2849, 1693, 1585, 1555, 1509, 1464, 1449, 1374, 1330, 1294, 1224, 1187, 1149, 1095, 1035, 964, 942, 872, 817, 734. Purity: 97.8% (Method B).

Biological Assay Protocols

General Information—Protocols for general cell culture, qPCR and Hh inhibition in C3H10T1/2 and ASZ cells are as previously described.²⁸ Protocols for the initiation and growth of Math1-Cre-ER;Ptc^{fl/fl} medulloblastoma tumors, isolation and in vitro culture of MERP MB cells, as well as the anti-proliferation and qPCR studies performed in these cells were as previously described.³²⁻³⁴ Sonic Hedgehog (C25II) recombinant mouse protein was purchased from Life Technologies. Data was analyzed using GraphPad Prism 5 and reported values represent mean \pm SEM for at least two separate experiments performed in triplicate.

HUVEC Cell Viability and Proliferation—HUVEC cell proliferation was assessed by measuring cellular metabolic activity using standard MTS/PMS protocols according to manufacturer's instructions. Briefly, HUVECs (3,000 cells/well) were seeded in a 96-well plate and allowed to attach overnight. Cells were treated with varying concentrations of drug as indicated and proliferation was assessed after 72 h with MTS.

Tube Formation Assay—Matrigel (BD Biosciences) was diluted 1:1 with DMEM (matrigel protein concentration no less than 3 mg/ml) and used to coat the wells of a 24-well tissue culture dish (280uL per well). Plates were incubated at 37°C for no more than 1 h until the matrigel solidified. HUVECs were suspended in M199 media with 1% FBS and penicillin/streptomycin and 50,000 cells were added to each well. Plates were incubated at 37°C for 20-30 min to allow HUVECs to attach to the matrigel. Cells were treated with control (DMSO), known angiogenic inhibitor suramin (10uM), or varying doses (10, 1, 0.1 μM) of drug and incubated for 16 h. Phase contrast images were taken from multiple locations in each well (8/well) on an inverted microscope and tube formation parameters quantified using Image J software (NIH).

Supplementary Material

Refer to Web version on PubMed Central for supplementary material.

Acknowledgments

We gratefully acknowledge support of this work by the National Institutes of Health/National Cancer Institute (CA190617) and the University of Connecticut Research Foundation (undergraduate research support for K.A.C. and D.S.R). ASZ001 cells were provided by Dr. Ervin Epstein (Children's Hospital Oakland Research Institute). We thank Victor W. Day at the University of Kansas for his small molecule crystallography work as well as the NSF-MRI (CHE-0923449) for their financial support of the x-ray diffractometer and software used in this study.

References

1. Kim J, Tang JY, Gong R, Kim J, Lee JJ, Clemons KV, Chong CR, Chang KS, Fereshteh M, Gardner D, Reya T, Liu JO, Epstein EH, Stevens DA, Beachy PA. Itraconazole, a commonly used antifungal that inhibits hedgehog pathway activity and cancer growth. *Cancer Cell*. 2010; 17:388–399. [PubMed: 20385363]
2. Chong CR, Xu J, Lu J, Bhat S, Sullivan DJ Jr, Liu JO. Inhibition of Angiogenesis by the Antifungal Drug Itraconazole. *ACS Chem Biol*. 2007; 2:263–270. [PubMed: 17432820]
3. Odds FC, Brown AJP, Gow NAR. Antifungal agents: mechanisms of action. *Trends Microbiol*. 2003; 11:272–279. [PubMed: 12823944]
4. Briscoe J, Théron PP. The mechanisms of hedgehog signaling and its roles in development and disease. *Nat Rev Mol Cell Biol*. 2013; 14:416–429. [PubMed: 23719536]
5. Amayke D, Jagani Z, Dorsch M. Unraveling the therapeutic potential of the hedgehog pathway in cancer. *Nat Med*. 2013; 19:1410–1422. [PubMed: 24202394]
6. Link G, Ahmadian A, Persson A, Undén AB, Afink G, Williams C, Uhlén M, Toftgård R, Lundeberg J, Pontén. PATCHED and p53 gene alterations in sporadic and hereditary basal cell carcinoma. *Oncogene*. 2001; 20:7770–7778. [PubMed: 11753655]
7. Reifemberger J, Wolter M, Knobbe CB, Köhler, Schönicke A, Scharwächter C, Kumar K, Blaschke B, Ruzicka T, Reifemberger G. Somatic mutations in the PTCH, SMOH, SUFUH, and TP53 genes in sporadic basal cell carcinoma. *Br J Dermatol*. 2005; 152:43–51. [PubMed: 15656799]
8. Gibson P, Tong Y, Robinson G, Thompson MC, Currie DS, Eden C, Kranenburg TA, Hogg T, Poppleton H, Martin J, Finkelstein D, Pounds S, Weiss A, Patay Z, Scoggins M, Ogg R, Pei Y, Yang ZJ, Brun S, Lee Y, Zindy F, Lindsey JC, Taketo MM, Boop FA, Sanford RA, Gajjar A, Clifford SC, Roussel MF, McKinnon PJ, Gutmann DH, Ellison DW, Wechsler-Reya R, Gilbertson RJ. Subtypes of medulloblastoma have distinct developmental origins. *Nature*. 2010; 468:1095–1099. [PubMed: 21150899]
9. Banerjee U, Hadden MK. Recent advances in the design of Hedgehog pathway inhibitors for the treatment of malignancies. *Expert Opin Drug Discov*. 2014; 9(7):751–771. [PubMed: 24850423]
10. Sharpe HJ, Wang W, Hannoush RN, de Sauvage FJ. Regulation of the oncoprotein smoothed by small molecules. *Nat Chem Biol*. 2015; 11:246–255. [PubMed: 25785427]
11. Shojaei F. Anti-angiogenesis therapy in cancer: current challenges and future perspectives. *Cancer Lett*. 2012; 320:130–137. [PubMed: 22425960]
12. Kerbel RS. Tumor angiogenesis. *New Engl J Med*. 2008; 358:2039–2049. [PubMed: 18463380]
13. Wahl O, Oswald M, Tretzel L, Herres E, Arend J, Efferth T. Inhibition of tumor angiogenesis by antibodies, synthetic small molecules and natural products. *Curr Med Chem*. 2011; 18:3136–3155. [PubMed: 21671856]
14. Yoo SY, Kwon SN. Angiogenesis and its therapeutic opportunities. *Mediators of Inflammation*. 2013 Article ID 127170.
15. Feng X. Angiogenesis and Antiangiogenesis Therapies: Spear and Shield of Pharmacotherapy. *J Pharma Care Health Sys*. 2014; 1(3)
16. Ferrara N, Kerbel RS. Angiogenesis as a therapeutic agent. *Nature*. 2005; 438:967–974. [PubMed: 16355214]
17. Prentice AG, Glasmacher A. Making sense of itraconazole pharmacokinetics. *J Antimicrob Chemother*. 2005; (Suppl. S1):i17–i22. [PubMed: 16120630]
18. Kumar S, Shen J, Burgess DJ. Nano-amorphous spray dried powder to improve oral bioavailability of itraconazole. *J Control Release*. 2014; 192:95–102. [PubMed: 25009979]
19. McEvoy GK, Snow EK. AHFS: Drug Information Bethesda MD American Society of Health-System Pharmacists. 2008
20. Odds FC, Brown AJP, Gow NAR. Antifungal agents: mechanisms of action. *Trends in Micro*. 2003; 11:272–279.
21. Isoherranen N, Kunze KL, Allen KE, Nelson WL, Thummel KE. Role of itraconazole metabolites in CYP3A4 inhibition. *Drug Metab Disp*. 2004; 32:1121–1131.

22. Ji H, Zhang W, Zhou Y, Zhang M, Zhu J, Song Y, Lü J, Zhu J. A three-dimensional model of lanosterol 14 α -demethylase of *Candida albicans* and its interactions with azole antifungals. *J Med Chem.* 2000; 43:2493–2505. [PubMed: 10891108]
23. Castro-Puyana M, Crego AL, Marina ML. Separation and quantitation of the four stereoisomers of itraconazole in pharmaceutical formulations by electrokinetic chromatography. *Electrophoresis.* 2006; 27:887–895. [PubMed: 16411272]
24. Shi W, Nacev BA, Aftab BT, Head S, Rudin CM, Liu JO. Itraconazole side chain analogues: Structure-activity relationship studies for inhibition of endothelial cell proliferation, vascular endothelial growth factor receptor 2 (VEGFR2) glycosylation, and hedgehog signaling. *J Med Chem.* 2011; 54:7363–7374. [PubMed: 21936514]
25. Shi W, Nacev BA, Bhat S, Liu JO. Impact of Absolute Stereochemistry on the Antiangiogenic and Antifungal Activities of Itraconazole. *ACS Med Chem Lett.* 2010; 1(4):155–159. [PubMed: 21892383]
26. Heeres J, Backx LJJ, Van Cutsem J. Antimycotic Azoles. 7. Synthesis and Antifungal Properties of a Series of Novel Triazol-3-ones. *J Med Chem.* 1984; 27:894–900. [PubMed: 6330360]
27. Baji H, Kimny T, Gasquez F, Flammang M, Compagnon PL, Delcourt A, Mathieu G, Viossat B, Morgant G, Nguyen-Huy D. Synthesis, antifungal activity and structure-activity relationships of 2-(alkyl or aryl)-2-(alkyl or polyazol-1-ylmethyl)-4-(polyazol-1-ylmethyl)-1,3-dioxolanes. *Eur J Med Chem.* 1997; 32:637.
28. Banerjee U, Ghosh M, Hadden MK. Evaluation of vitamin D3 A-ring analogues as hedgehog pathway inhibitors. *Bioorg Med Chem Lett.* 2012; 22:1330–1334. [PubMed: 22226657]
29. Arnaoutova I, Kleinman HK. In vitro angiogenesis: endothelial cell tube formation on gelled basement membrane extract. *Nat Protoc.* 2010; 5:628–635. [PubMed: 20224563]
30. So PL, Langston AW, Daniellinia N, Hebert JL, Fujimoto MA, Khaimskiy Y, Aszterbaum M, Epstein EH. Long-term establishment, characterization and manipulation of cell lines from mouse basal cell carcinoma tumors. *Exp Dermatol.* 2006; 15:742–750. [PubMed: 16881970]
31. Tang JY, Xiao TZ, Oda Y, Chang KS, Shpall E, Wu A, So PL, Hebert J, Bikle D, Epstein EH. Vitamin D3 inhibits hedgehog signaling and proliferation in murine basal cell carcinomas. *Cancer Prev Res.* 2011; 4:744–751.
32. Yang ZJ, Ellis T, Markant SL, Read TA, Kessler JD, Bourboulas M, Schüller U, Machold R, Fishell G, Rowitch DH, Wainwright BJ, Wechsler-Reya RJ. Medulloblastoma can be initiated by deletion of *Patched* in lineage-restricted progenitors or stem cells. *Cancer Cell.* 2008; 14:135–145. [PubMed: 18691548]
33. Markant SL, Esparza LA, Sun J, Barton KL, McCoig LM, Grant GA, Crawford JR, Levy ML, Northcott PA, Shih D, Remke M, Taylor MD, Wechsler-Reya RJ. Targeting sonic hedgehog-associated medulloblastoma through inhibition of Aurora and Polo-like kinases. *Cancer Res.* 2013; 73:6310–6322. [PubMed: 24067506]
34. Brun SN, Markant SL, Esparza LA, Garcia G, Terry D, Huang JM, Pavlyukov MS, Li XN, Grant GA, Crawford JR, Levy ML, Conway EM, Smith LH, Nakano I, Berezov A, Greene MI, Wang Q, Wechsler-Reya RJ. Survivin as a therapeutic target in Sonic hedgehog-driven medulloblastoma. *Oncogene.* 2015; 34:3770–3779. [PubMed: 25241898]
35. Tanoury GJ, Hett R, Wilkinson HS, Wald SA, Senanayake CH. Total synthesis of (2*R*, 4*S*, 2'*S*, 3'*R*)-hydroxyitraconazole: implementations of a recycle protocol and a mild and safe phase-transfer reagent for preparation of the key chiral units. *Asymmetry.* 2003; 14:3487–3493.
36. Yauch RL, Dijkgraaf GJ, Aliche B, Januario T, Ahn CP, Holcomb T, Pujara K, Stinson J, Callahan CA, Tang T, Bazan JF, Kan Z, Seshagiiri S, Hann CL, Gould SE, Low JA, Rudin CM, de Sauvage FJ. Smoothed mutation confers resistance to a hedgehog pathway inhibitor in medulloblastoma. *Science.* 2009; 326:572–574. [PubMed: 19726788]
37. Dijkgraaf GJP, Aliche B, Weinmann L, Januario T, West K, Modrusan Z, Burdick D, Goldsmith R, Robarge K, Sutherland D, Scales SJ, Gould SE, Yauch RL, de Sauvage FJ. Small molecule inhibition of GDC-0449 refractory smoothed mutants and downstream mechanisms of drug resistance. *Cancer Res.* 2011; 71:435–444. [PubMed: 21123452]

38. Priol S, Cartelazzi B, Col VD, Marson D, Laurini E, Fermeglia M, Licitra L, Pilotti S, Bossi P, Perrone F. Smoothened (SMO) receptor mutations dictate resistance to vismodegib in basal cell carcinoma. *Mol Oncol*. 2015; 9:389–397. [PubMed: 25306392]
39. Sharpe HJ, Pau G, Dijkgraaf GJ, Basset-Seguín N, Modrusan Z, Januario T, Tsui V, Durham AB, Dlugosz AA, Haverty PM, Bourgon R, Tang JY, Sarin KY, Dirix L, Fisher DC, Rudin CM, Sofen H, Migden MR, Yauch RL, de Sauvage FJ. Genomic analysis of smoothened inhibitor resistance in basal cell carcinoma. *Cancer Cell*. 2015; 27:327–341. [PubMed: 25759019]
40. Atwood SX, Sarin KY, Whitson RJ, Li JR, Kim G, Rezaee M, Ally MS, Kim J, Yao C, Chang ALS, Oro AE, Tang JY. Smoothened variants explain the majority of drug resistance in basal cell carcinoma. *Cancer Cell*. 2015; 27:342–353. [PubMed: 25759020]
41. Kim J, Aftab BT, Tang JY, Kim D, Lee AH, Rezaee M, Kim J, Chen B, King EM, Borodovsky A, Riggins GJ, Epstein EH, Beachy PA, Rudin CM. Itraconazole and arsenic trioxide inhibit hedgehog pathway activation and tumor growth associated with acquired resistance to smoothened antagonists. *Cancer Cell*. 2013; 23:23–34. [PubMed: 23291299]
42. Maschinot CA, Pace JR, Hadden MK. Small molecule synthetic inhibitors of Hh signaling as anti-cancer chemotherapeutics. *Curr Med Chem*. 2015

Abbreviations

ITZ	itraconazole
Hh	Hedgehog
Gli	glioblastoma associated oncogene
Ptch	patched
MEF	mouse embryonic fibroblast

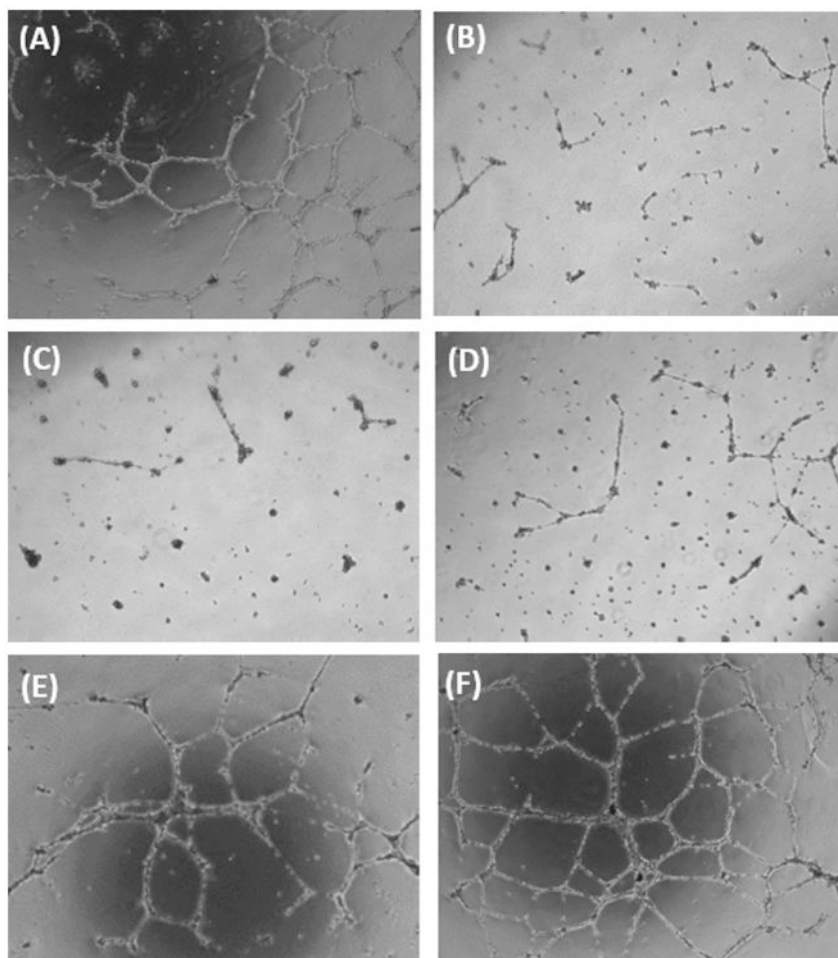


Figure 1. Tube formation assays for ITZ and its analogues. (A) DMSO, (B) Suramin, (C) ITZ, (D) **2**, (E) **18**, (F) **21**. All compounds were evaluated at 10 μ M and each image is a representative visual field from a single assay. Each assay was repeated at least three distinct times.

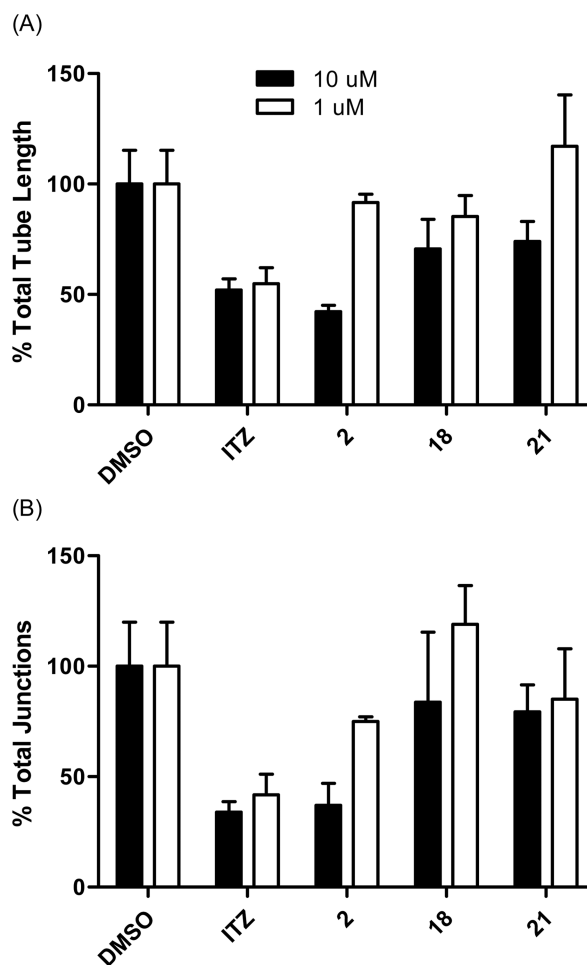
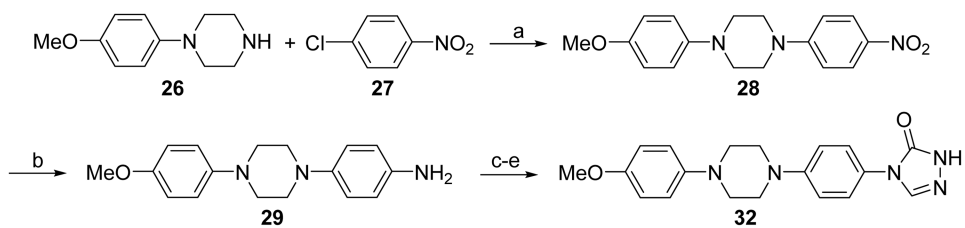
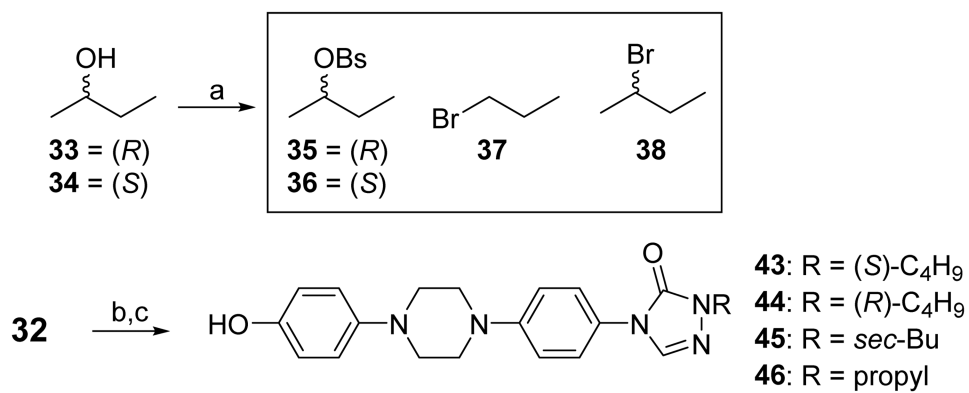


Figure 2. Comparison of total tube length (A) and total tube junctions (B) for ITZ, **2**, **18**, and **21**. DMSO (negative control) was set as 100% tube formation for analysis purposes. Suramin (10 μ M) was used as the positive control for each experiment and its ability to inhibit tube length ($51.9 \pm 7.8\%$) and tube junctions ($57.6 \pm 6.1\%$) was consistent. Data represent the Ave \pm SEM of at least 3 separate experiments in which 5 fields of vision were quantified using ImageJ software.

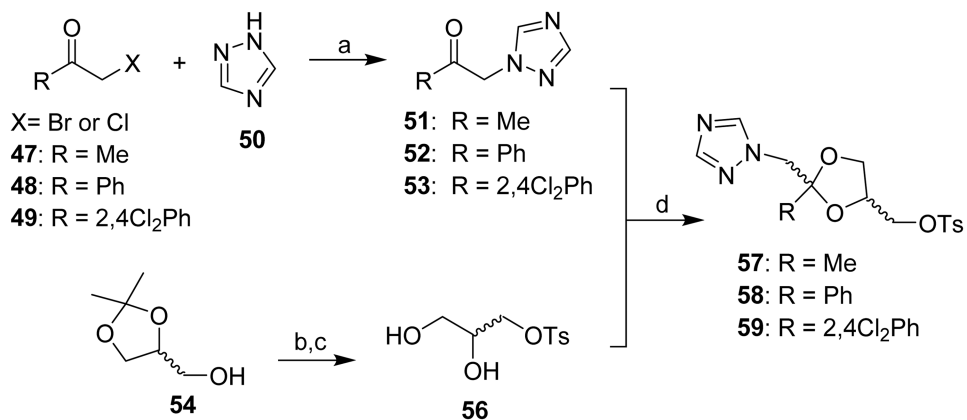
**Scheme 1.**Synthesis of linker region intermediate.^a

^aReagents and conditions: (a) K_2CO_3 , reflux, 12 h, 82%; (b) Pd/C, $NH_2NH_2 \cdot H_2O$ (10 eq), reflux, 3.5 h, 71%; (c) Pyr (17 eq), ClCOOPh (1.1 eq), 3 h, 90%; (d) $NH_2NH_2 \cdot H_2O$ (5.5 eq), reflux, 3 h, quant; (e) formamidine acetate (4.5 eq), acetic acid, reflux, 3 h, 91%.

**Scheme 2.**

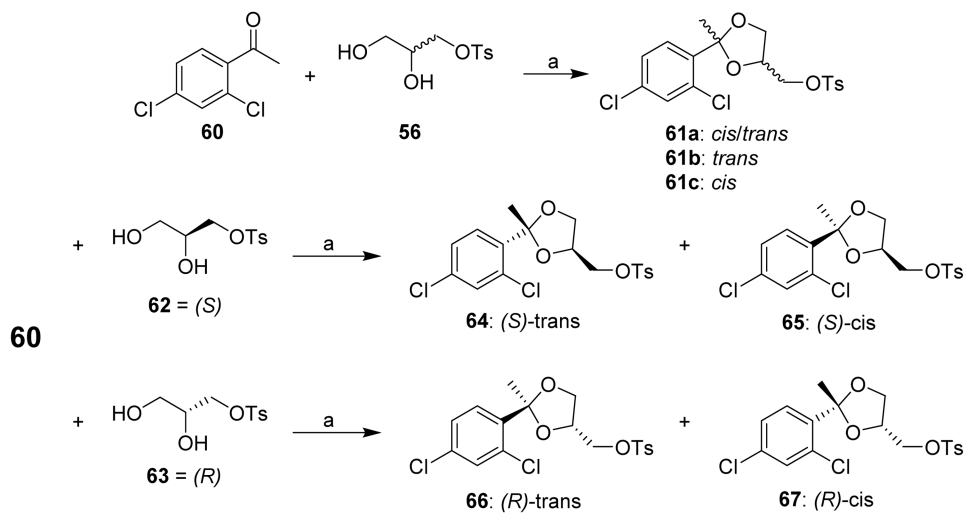
Synthesis of linker/triazolone/side chain intermediates.^a

^aReagents and conditions: (a) Et₃N, BsCl (1.3 eq), RT, 3 h; 30-50%; (b) Cs₂CO₃, brosyl/bromo alkyl chain, RT, 12 h, 45-88% (c) 48% HBr, toluene, reflux, 12 h, 55-80%.

**Scheme 3.**

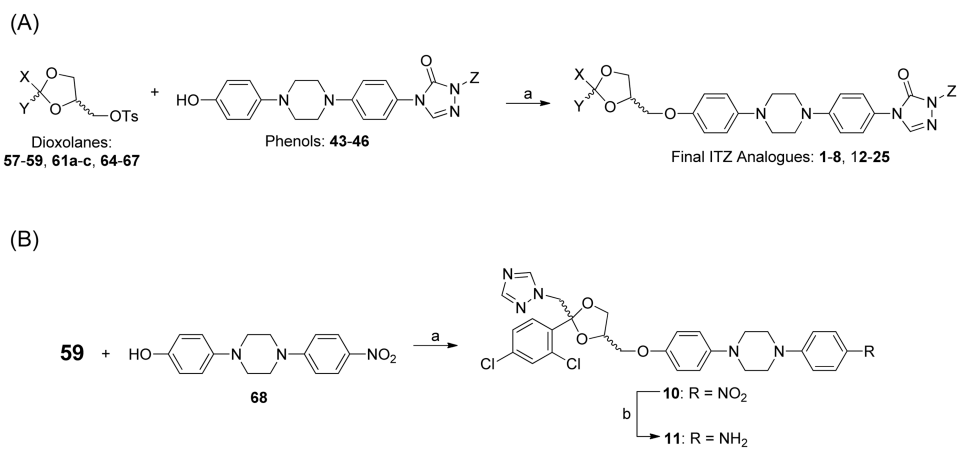
Synthesis of triazole-containing dioxolane region intermediates.^a

^aReagents and conditions: (a) NaHCO₃, toluene, reflux, 3h, 25-65%; (b) Pyr, TsCl, 0°C- RT, 12 h, 71%; (c) MeOH, 0.5N HCl, reflux, 5 h, 89%; (d) Triflic acid (3-4 eq), toluene, RT, 60 h 10-70%.

**Scheme 4.**

Synthesis of *des*-triazole dioxolane region intermediates.^a

^aReagents and conditions: (a) p-TsOH (cat.), toluene, reflux (Dean Stark), 48 h, 70-90%.

**Scheme 5.**Coupling reactions for final ITZ analogues.^a

^aReagents and conditions: (a) Cs₂CO₃ (10 eq), DMSO, 90°C, 12 h, 45-88%; (b) Pd/C, NH₂NH₂•H₂O (10 eq), reflux, 3.5 h, 60-70%. The functional groups represented by X, Y, and Z above can be found in Schemes 2-4.

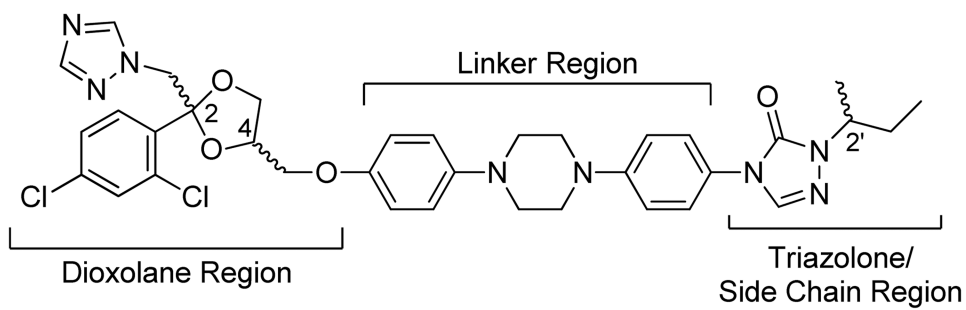
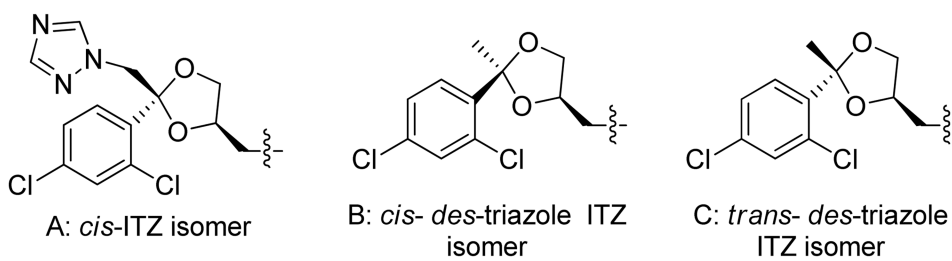


Chart 1.
Structure and regions of itraconazole (ITZ).

**Chart 2.**

Cis- and *trans*- nomenclature of dioxolane region: (A) representative *cis*-ITZ isomer, (B) *cis*- and (C) *trans*-*des*-triazole analogues.

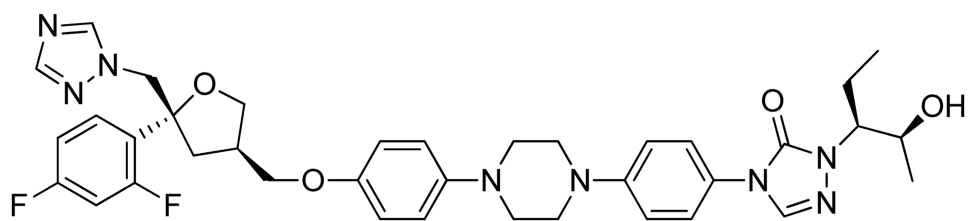


Chart 3.
Structure of posaconazole (PSZ).

Table 1

First generation series of ITZ analogues.

Compound	R1	R2	R3
1, ITZ			
2	-CH ₃		
3			
4		-CH ₃	
5	-CH ₃	-CH ₃	
6			
7			

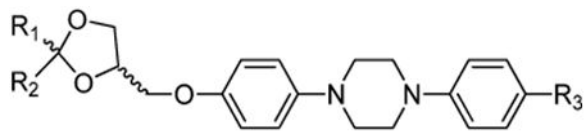
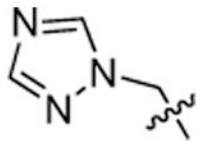
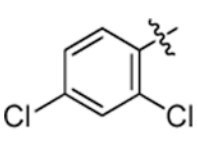
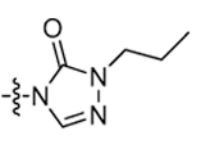
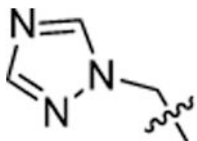
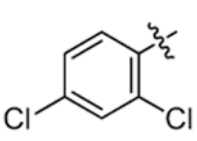
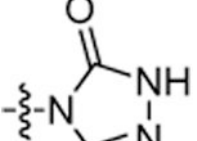
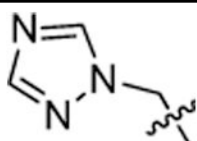
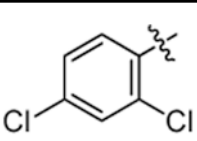
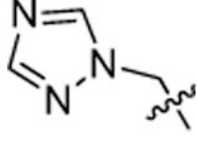
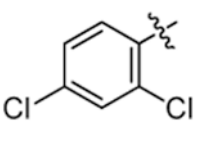
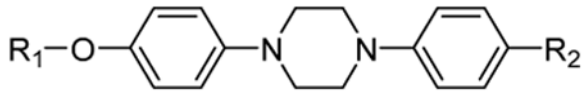
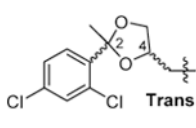
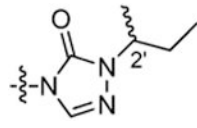
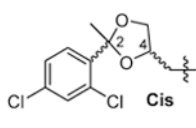
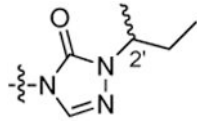
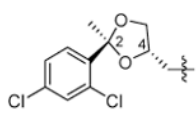
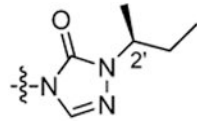
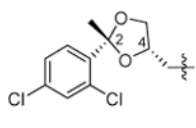
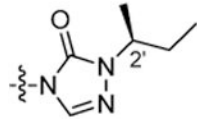
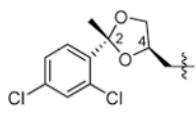
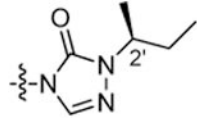
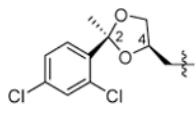
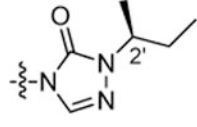
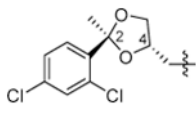
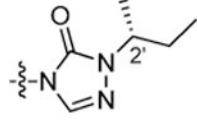
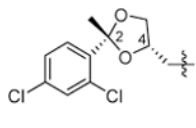
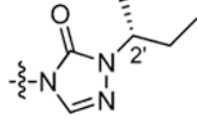
			
Compound	R1	R2	R3
8			
9			
10			-NO ₂
11			-NH ₂

Table 2Second generation, stereochemically defined analogues of **2**.

			
Compound	R1	R2	Final Stereochemistry
12	 Trans		<i>Trans</i> -2,4
13	 Cis		<i>Cis</i> -2,4
14			<i>Trans</i> -2 <i>S</i> ,4 <i>S</i> ,2' <i>S</i>
15			<i>Cis</i> -2 <i>R</i> ,4 <i>R</i> ,2' <i>S</i>
16			<i>Trans</i> -2 <i>R</i> ,4 <i>R</i> ,2' <i>S</i>
17			<i>Cis</i> -2 <i>S</i> ,4 <i>R</i> ,2' <i>S</i>
18			<i>Trans</i> -2 <i>S</i> ,4 <i>S</i> ,2' <i>R</i>
19			<i>Cis</i> -2 <i>R</i> ,4 <i>S</i> ,2' <i>R</i>

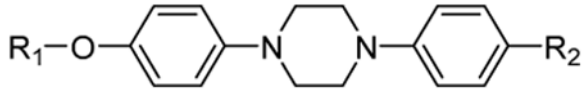
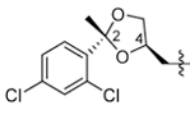
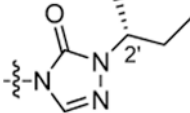
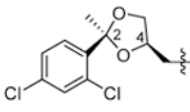
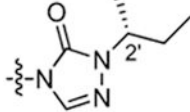
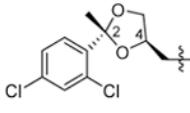
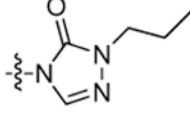
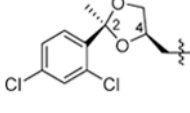
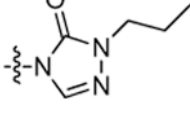
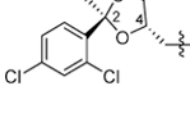
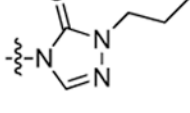
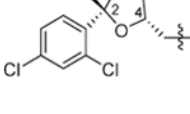
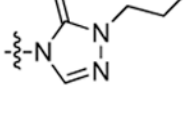
			
Compound	R1	R2	Final Stereochemistry
20			<i>Trans</i> -2R,4R,2'R
21			<i>Cis</i> -2S,4R,2'R
22			<i>Trans</i> -2R,4R
23			<i>Cis</i> -2S,4R
24			<i>Trans</i> -2S,4S
25			<i>Cis</i> -2R,4S

Table 3

In vitro activity of first generation ITZ analogues.

Compound	% Gli expression (1 μ M) ^d	IC ₅₀ (μ M) ^c		ASZ ^d	GI ₅₀ (μ M) ^c HUYEC	GI ₅₀ (μ M) ^c MERP MB ^d
		C3H10T1/2 ^a	ASZ ^d			
ITZ	---	0.074 \pm 0.02	0.14 \pm 0.02		0.40 \pm 0.03	0.44 \pm 0.08
1	1.7 \pm 0.3 ^b	0.063 \pm 0.003	0.17 \pm 0.01		0.49 \pm 0.09	0.6 \pm 0.1
2	17.8 \pm 0.5	0.14 \pm 0.04	0.17 \pm 0.04		23.8 \pm 6.7	ND
3	13.1 \pm 1.2	0.42 \pm 0.2	0.45 \pm 0.06		8.3 \pm 0.7	ND
4	61.4 \pm 3.5	ND	ND		18.4 \pm 4.5	ND
5	71.4 \pm 5.5	ND	ND		>100	ND
6	6.9 \pm 3.1	0.16 \pm 0.04	0.14 \pm 0.008		2.5 \pm 0.3	ND
7	3.0 \pm 0.9	0.14 \pm 0.04	0.16 \pm 0.07		1.7 \pm 0.4	ND
8	58.5 \pm 6.4	ND	ND		4.7 \pm 0.3	ND
9	1.1 \pm 0.2	0.043 \pm 0.02	0.12 \pm 0.03		5.8 \pm 0.8	ND
10	1.5 \pm 0.05	0.13 \pm 0.03	0.09 \pm 0.01		8.4 \pm 0.7	ND
11	6.1 \pm 1.6	0.16 \pm 0.06	0.12 \pm 0.05		42.7 \pm 4.4	0.9 \pm 0.7
45	45.7 \pm 3.0	ND	ND		>100	ND

^a All analogues evaluated following 24 hr incubation.

^b Values represent %Gli1 expression relative to recombinant Hh ligand control (set as 100%).

^c IC₅₀ and GI₅₀ values represent the Mean \pm SEM of at least two separate experiments performed in triplicate.

^d All analogues evaluated following 48 hr incubation.

Table 4

In vitro activity of second generation ITZ analogues.

Compound	IC ₅₀ (μM) ^a		GI ₅₀ (μM) ^a	GI ₅₀ (μM) ^a
	C3H10T1/2 ^b	ASZ ^c	HUVEC	MERPMB ^c
12	0.091 ± 0.02	0.077 ± 0.01	3.32 ± 0.55	2.0 ± 1.3
13	0.85 ± 0.1	0.071 ± 0.02	3.69 ± 1.1	2.9 ± 1.9
14	1.1 ± 0.17	2.5 ± 0.7	7.7 ± 4.4	ND
15	>10	0.55 ± 0.07	78.3 ± 17.3	ND
16	0.47 ± 0.001	0.38 ± 0.07	18.3 ± 11.8	ND
17	1.85 ± 0.09	0.15 ± 0.038	2.5 ± 0.7	0.39 ± 0.2
18	0.54 ± 0.24	0.13 ± 0.04	12.1 ± 4.7	ND
19	6.6 ± 0.3	2.8 ± 0.9	65.0 ± 11.5	ND
20	0.19 ± 0.04	0.022 ± 0.01	53.2 ± 25.2	0.6 ± 0.2
21	2.4 ± 0.6	0.024 ± 0.02	12.8 ± 2.9	1.0 ± 0.5
22	4.1 ± 1.5	1.3 ± 0.65	26.5 ± 3.5	ND
23	>10	1.4 ± 0.5	49.9 ± 15.9	ND
24	>10	0.2 ± 0.08	84.1 ± 33.5	22.4 ± 12
25	>10	0.54 ± 0.06	24.9 ± 2.2	ND
PSZ	0.14 ± 0.02	0.54 ± 0.05	1.6 ± 0.02	1.5 ± 0.3

^aIC₅₀ and GI₅₀ values represent the Mean ± SEM of at least two separate experiments performed in triplicate.^bAll analogues evaluated following 24 hr incubation.^cAll analogues evaluated following 48 hr incubation.

Table 5

Down-regulation of Gli1 mRNA in MERP MB cells.

Compound ^a	IC ₅₀ (μM) ^b
ITZ	0.39 ± 0.06
17	0.26 ± 0.12
20	0.19 ± 0.07
21	0.29 ± 0.08

^aAll analogues evaluated following 48 hr incubation.^bIC₅₀ values represent the Mean ± SEM of two separate experiments.